



DUDLEY KNOX LIBRARY
NAVAL POSTGRADUATE SCHOOL
MONTEREY CA 93943-5101

Approved for public release; distribution is unlimited.

Measurement and Prediction of the Flow
Through an Annular Turbine Cascade

by

Gregory D. Thomas
Lieutenant, United States Navy
B.S., Colorado School of Mines, 1985

Submitted in partial fulfillment
of the requirements for the degree of

MASTER OF SCIENCE IN AERONAUTICAL ENGINEERING

from the

NAVAL POSTGRADUATE SCHOOL
June 1993

~~Department of Aeronautics and Astronautics~~

REPORT DOCUMENTATION PAGE

1a Report Security Classification: Unclassified		1b Restrictive Markings	
2a Security Classification Authority		3 Distribution/Availability of Report	
2b Declassification/Downgrading Schedule		Approved for public release; distribution is unlimited.	
4 Performing Organization Report Number(s)		5 Monitoring Organization Report Number(s)	
6a Name of Performing Organization Naval Postgraduate School	6b Office Symbol (if applicable) 31	7a Name of Monitoring Organization Naval Postgraduate School	
6c Address (city, state, and ZIP code) Monterey CA 93943-5000		7b Address (city, state, and ZIP code) Monterey CA 93943-5000	
8a Name of Funding/Sponsoring Organization	6b Office Symbol (if applicable)	9 Procurement Instrument Identification Number	
Address (city, state, and ZIP code)		10 Source of Funding Numbers	
		Program Element No	Project No
		Task No	Work Unit Accession
11 Title (include security classification) MEASUREMENT AND PREDICTION OF THE FLOW THROUGH AN ANNULAR TURBINE CASCADE			
12 Personal Author(s) GREGORY DAVID THOMAS			
13a Type of Report Master's Thesis	13b Time Covered From To	14 Date of Report (year, month, day) 1993 JUNE 2	15 Page Count 82
16 Supplementary Notation The views expressed in this thesis are those of the author and do not reflect the official policy or position of the Department of Defense or the U.S. Government.			
17 Cosati Codes		18 Subject Terms (continue on reverse if necessary and identify by block number)	
Field	Group	RVC3D, NUMERICAL SIMULATION, TURBINE, LDV, CASCADE	
	Subgroup		
19 Abstract (continue on reverse if necessary and identify by block number) An annular turbine cascade was designed and manufactured for laser Doppler velocimetry and probe measurements in a small-scale rig. The purpose of the experiment was to determine the limitations of these measurements in a confined annulus, and to compare the experimental results with numerical predictions. Downstream probe surveys were conducted at a Reynolds number of 50000. Total pressure and temperature measurements were taken upstream of the test section, and hub static pressure was measured downstream of the cascade. A two-dimensional laser anemometer was used to obtain preliminary velocity field measurements for code validation. The two main problem areas identified were the type of seeding material used and the configuration of the optical access window. Flowfield characteristics were predicted using a three-dimensional viscous code, which were then compared to experimental measurements. The comparison showed that the numerical simulator predicted well the general features of the flow field that were measured in the experiment. Recommendations are made which would improve the mapping of the velocity field for a more complete code validation.			
20 Distribution/Availability of Abstract __ unclassified/unlimited __ same as report __ DTIC users		21 Abstract Security Classification Unclassified	
22a Name of Responsible Individual GARTH V. HOBSON		22b Telephone (include Area Code) (408)656-2888	22c Office Symbol CODE 31

ABSTRACT

An annular turbine cascade was designed and manufactured for laser Doppler velocimetry and probe measurements in a small-scale rig. The purpose of the experiment was to determine the limitations of these measurements in a confined annulus, and to compare the experimental results with numerical predictions. Downstream probe surveys were conducted at a Reynolds number of 500000. Total pressure and temperature measurements were taken upstream of the test section, and hub static pressure was measured downstream of the cascade. A two-dimensional laser anemometer was used to obtain preliminary velocity field measurements for code validation. The two main problem areas identified were the type of seeding material used and the configuration of the optical access window. Flowfield characteristics were predicted using a three-dimensional viscous code, which were then compared to experimental measurements. The comparison showed that the numerical simulator predicted well the general features of the flow field that were measured in the experiment. Recommendations are made which would improve the mapping of the velocity field for a more complete code validation.

110315
T41533
C.1

TABLE OF CONTENTS

I. INTRODUCTION 1

II. EXPERIMENTAL SETUP 4

 A. APPARATUS 4

 B. COBRA PROBE MEASUREMENTS 10

 C. LASER SETUP 12

 D. EXPERIMENTAL PROCEDURE 16

III. NUMERICAL SIMULATION 17

 A. COMPUTATIONAL SCHEME 17

 B. GRID GENERATION 18

 1. GRID GENERATION COMPARISON 21

 2. RECOMMENDATIONS 22

IV. RESULTS AND DISCUSSION 23

 A. LASER DOPPLER VELOCIMETRY MEASUREMENTS 23

 B. NUMERICAL RESULTS 23

 C. COMPARISON OF DOWNSTREAM LOSSES AND EXIT FLOW
 ANGLES 28

V. CONCLUSIONS AND RECOMMENDATIONS 40

APPENDIX A.	SAMPLE INPUT FILES	42
APPENDIX B.	RVC3D USER'S GUIDE	48
APPENDIX C.	COBRA PROBE MEASUREMENTS	50
APPENDIX D.	DRAWINGS	59
APPENDIX E.	NUMERICAL SIMULATION OUTPUT	67
APPENDIX F.	LDV DATA	70
LIST OF REFERENCES	72
INITIAL DISTRIBUTION LIST	73

LIST OF FIGURES

Figure 1.	Schematic of ATC	5
Figure 2.	Blade geometry	6
Figure 3.	Planview of test apparatus	7
Figure 4.	Sideview of test apparatus	8
Figure 5.	Compressed air supply	9
Figure 6.	LDV measurement points	11
Figure 7.	LDV component schematic	13
Figure 8.	LDV processing hardware	15
Figure 9.	Grape grid	19
Figure 10.	3-D grid	20
Figure 11.	Probe location	24
Figure 12.	Blade surface static pressure	25
Figure 13.	Blade surface static pressure at mid-span	26
Figure 14.	Stagnation pressure on the exit plane	27
Figure 15.	Mach number comparison at 10% span	29
Figure 16.	Mach number comparison at 25% span	30
Figure 17.	Mach number comparison at 50% span	31
Figure 18.	Mach number comparison at 75% span	32
Figure 19.	Mach number comparison at 90% span	33
Figure 20.	Flow angle comparison at 10% span	35
Figure 21.	Flow angle comparison at 25% span	36
Figure 22.	Flow angle comparison at 50% span	37
Figure 23.	Flow angle comparison at 75% span	38

Figure 24. Flow angle comparison at 90% span 39

I. INTRODUCTION

The measurement of secondary flows in annular turbine cascades (ATC) is very important to gas turbine designers and computational fluid dynamicists. A decrease in stator performance caused by secondary flow has a significant effect on turbine stage performance. Therefore, the quantification of secondary flow effects on performance (i.e. losses) is particularly important for small aspect ratio core turbines.

The computational prediction of component performance is potentially a valuable tool for turbomachinery designers. A small improvement in engine efficiency can amount to huge savings in yearly fuel costs for a wing of aircraft. Good quantitative predictions of turbomachinery performance are necessary for turbomachinery designers to increase engine performance at a minimum cost.

This report presents the results of numerical simulation of an ATC and verification by experimental measurements. A cascade was designed and built by the author so that laser Doppler velocimetry (LDV) and probe measurements of turbine secondary flows could be performed. Three-hole probe measurements were taken in the wake of a high turning turbine nozzle. These were compared with the numerical

results obtained by running RVC3D, a three-dimensional, viscous, computer program.

The longer term goal of this research is to obtain LDV measurements as close as possible to the endwalls and to fully determine the flowfield structure in the presence of tip clearance effects.

Several researchers have investigated secondary flows in turbine cascades. Louis Goldman and Richard G. Seaholtz have published several papers on laser measurements in an annular cascade of high turning core turbine vanes [Ref. 1 & 2]. Their work consisted of making laser anemometer measurements in the blade passages, and limited measurements in the wake region. These measurements, along with blade surface static pressures, were compared to predictions made with a three-dimensional inviscid flow analysis program. The experimental measurements compared well with the calculated values. There was poor agreement however in the wake region where viscous effects dominated, which could not be resolved with the inviscid flow analysis program.

A. Yamamoto has also published several papers on secondary flows in turbine cascades. Reference 3 reports a detailed investigation of secondary flow/loss mechanisms. Five-hole probe measurements in two types of turbine cascades with different turning angles were presented. Yamamoto's work focused on complete flowfield surveys within the blade rows of linear turbine cascades.

Rodrick V. Chima developed a three-dimensional flow analysis code to compute the design, and off-design operating conditions in transonic rotors [Ref. 4]. His code, RVC3D, a computer code for analysis of three-dimensional viscous flows in turbomachinery, was used for the numerical prediction of the flows in the annular turbine cascade.

II. EXPERIMENTAL SETUP

A. APPARATUS

The experimental results were obtained using a transonic turbine stator tested in an annular cascade facility at the Turbopropulsion Laboratory of the Naval Postgraduate School. The schematic of the test rig can be seen in Figure 1. The hub and tip have constant radii with a hub radius of 3.89 in and a tip radius of 4.585 in. The tested cascade had 31 blades measuring 1.1 in high and 1.00 in axial chord, as can be seen in Figure 2. The blade spacing at mid-span was 0.86 inches. The blades were stacked radially, and there was no change in blade shape in the radial direction. The inflow was purely axial at an average Mach number of 0.13. The inlet total-to-exit hub static pressure ratio was 0.68, which gave an average exit Mach number of 0.59. The apparatus that housed the turbine can be seen in Figures 3 and 4.

Airflow was provided by a VA-312 Allis-Chalmers, 12-stage axial-flow compressor, operating at 12,000 rpm. The compressor produced a mass flow rate of 7.74 lb/sec, during the experiment. The piping schematic can be seen in Figure 5. The air entered the ten inch flange (Fig. 4) through a honeycomb flow straightener, after leaving the plenum

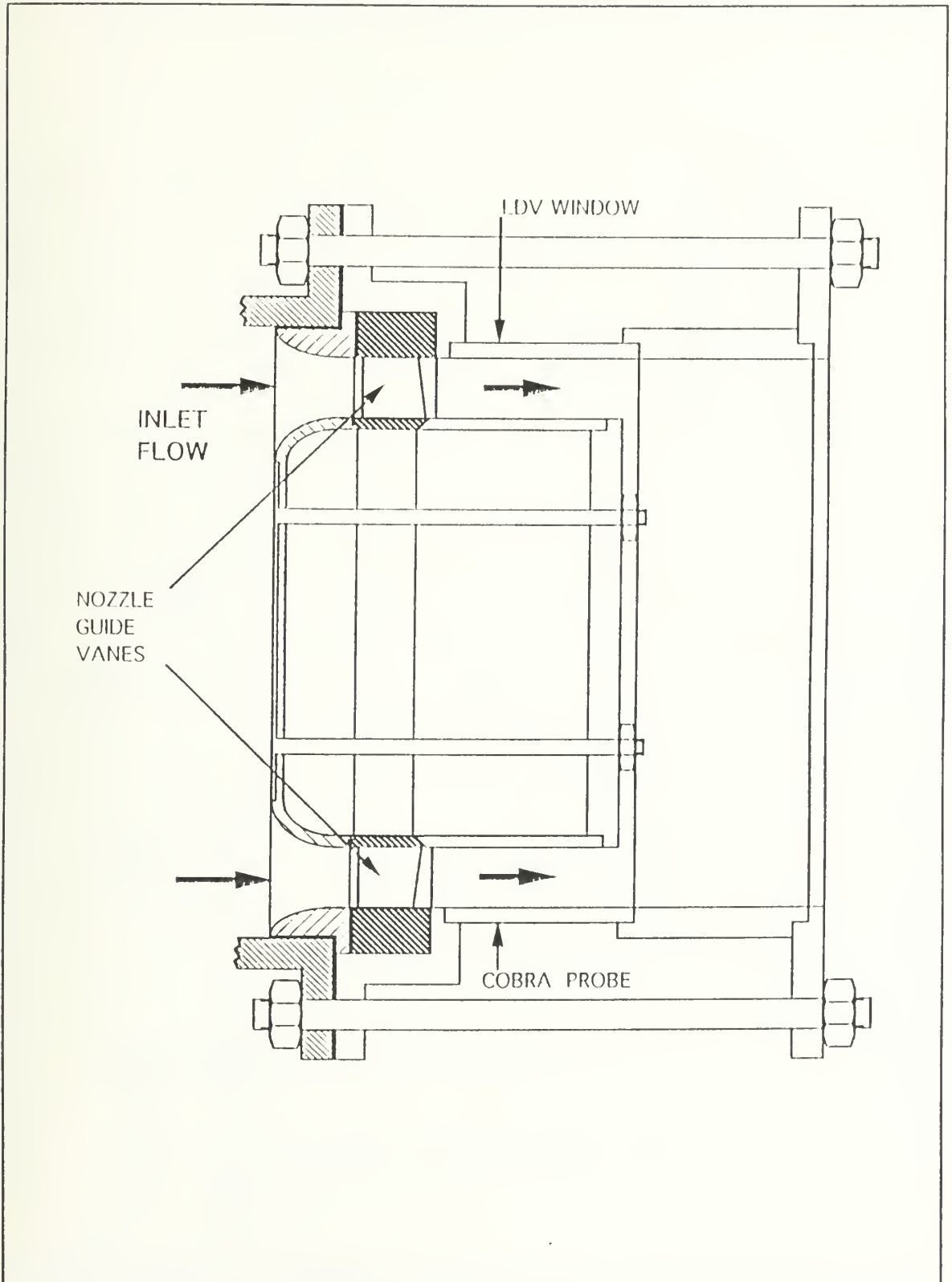
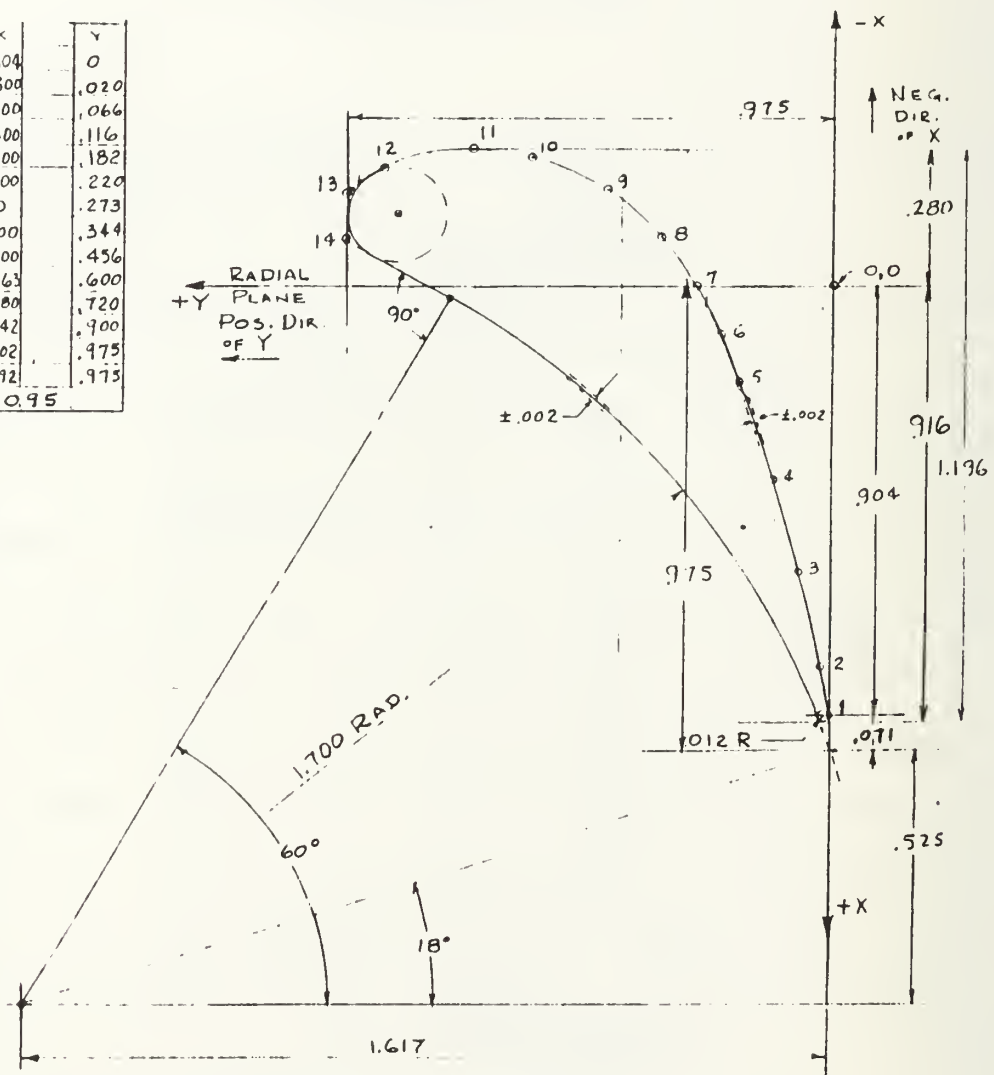


Figure 1. Schematic of ATC

POINT	X	Y
1	.104	0
2	.800	.020
3	.600	.066
4	.400	.116
5	.200	.182
6	.100	.220
7	0	.273
8	-.100	.344
9	-.200	.456
10	-.263	.600
11	-.280	.720
12	-.242	.900
13	-.202	.975
14	-.092	.975

L.E.R. = .095



SECTION PERPENDICULAR TO RADIAL PLANE
SCALE: $\frac{5}{1}$

NOTE: SAME PROFILE AT ALL RADII
BETWEEN 7.79 DIA. AND 9.17 DIA.

Figure 2. Blade geometry

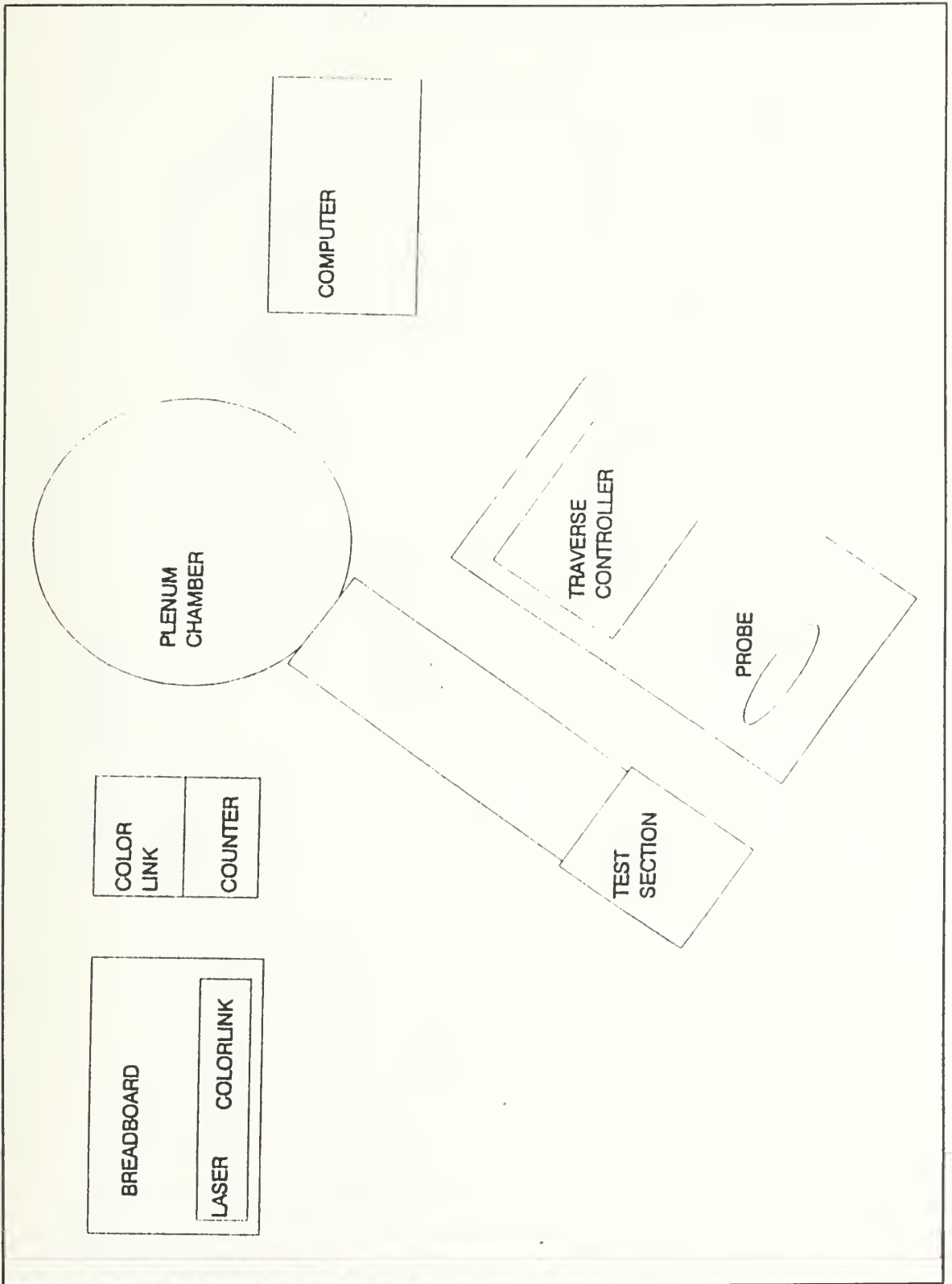


Figure 3. Planview of test apparatus

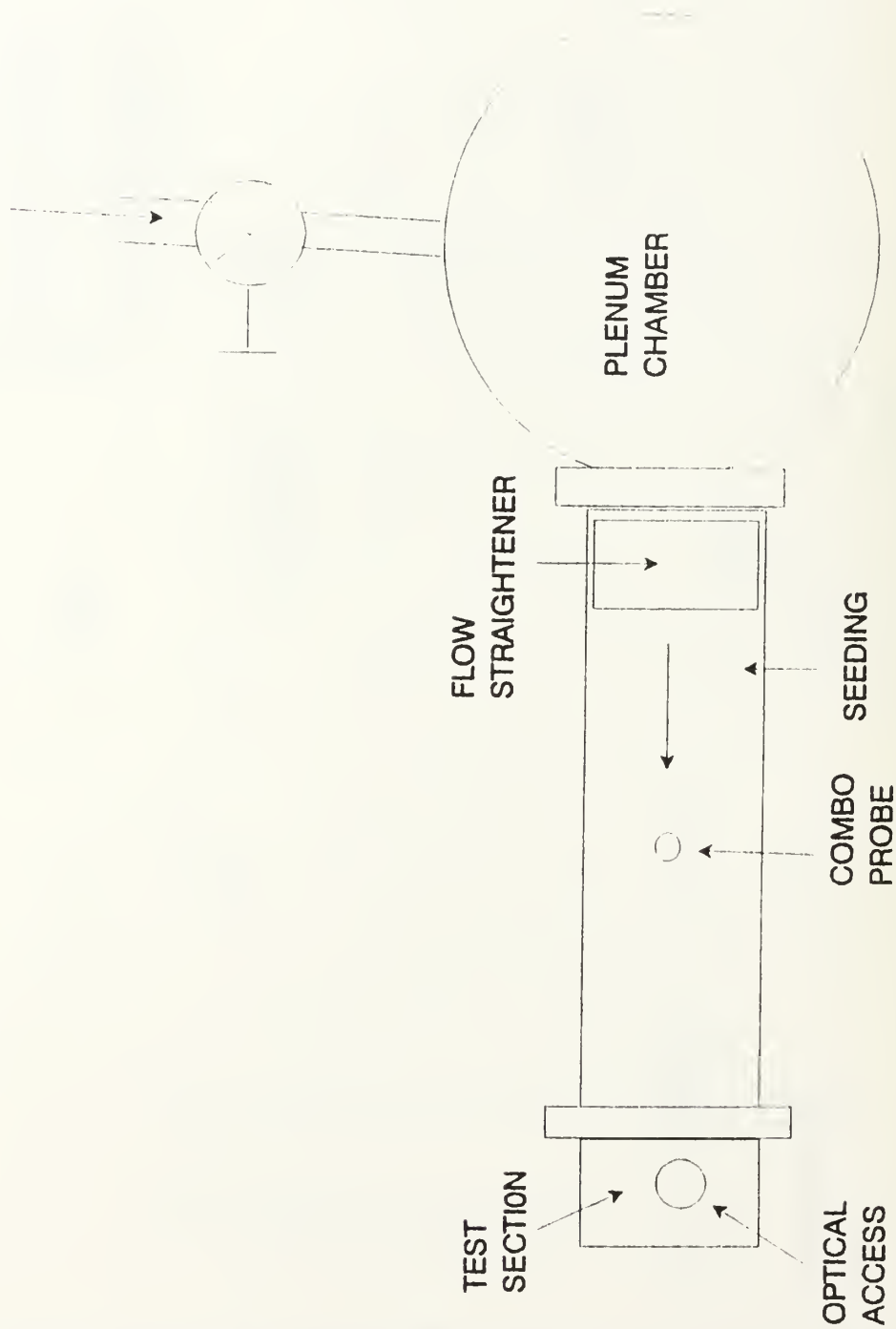


Figure 4. Sideview of test apparatus

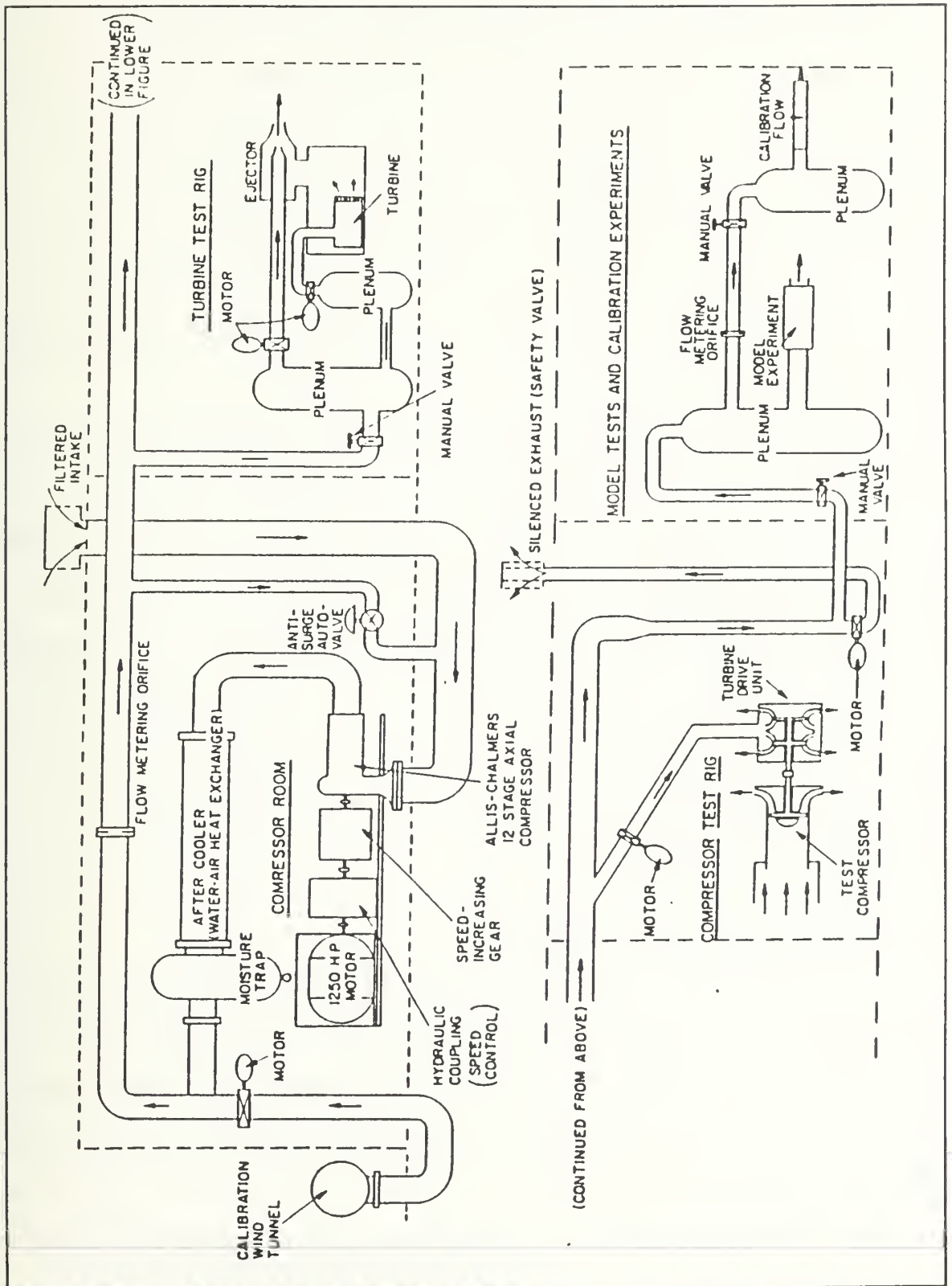


Figure 5. Compressed air supply

chamber. The air was then directed into the test section through the bellmouth, (Fig. 1) which smoothly reduced the airflow from a ten inch diameter to a 9.17 inch diameter section. After leaving the turbine blades the air was dumped three chord lengths beyond the blade row, on the inner-hub surface. The air was finally discharged at the outer tip surface, which was four chord lengths downstream, into the test cell.

Laser measurements were designed to be taken through an optical window which was centered two chords downstream from the trailing edge. As seen in Figure 6, the LDV measurement points were located downstream of the blades at different peripheral stations. These tangential surveys, at different radial locations, would cover a plane of data output from the numerical simulation. This was to allow direct comparison between the numerical simulation and the experimental results.

B. COBRA PROBE MEASUREMENTS

A cobra probe was used to measure the flowfield on the exit plane at various radii, and at the same axial location as the LDV measurements. The cobra probe measurements were taken at 10, 25, 50, 75, and 100 percent span, as measured from the hub.

The cobra probe was a three-hole probe, with the center hole 0.036 inches in diameter, and the two side ports set at

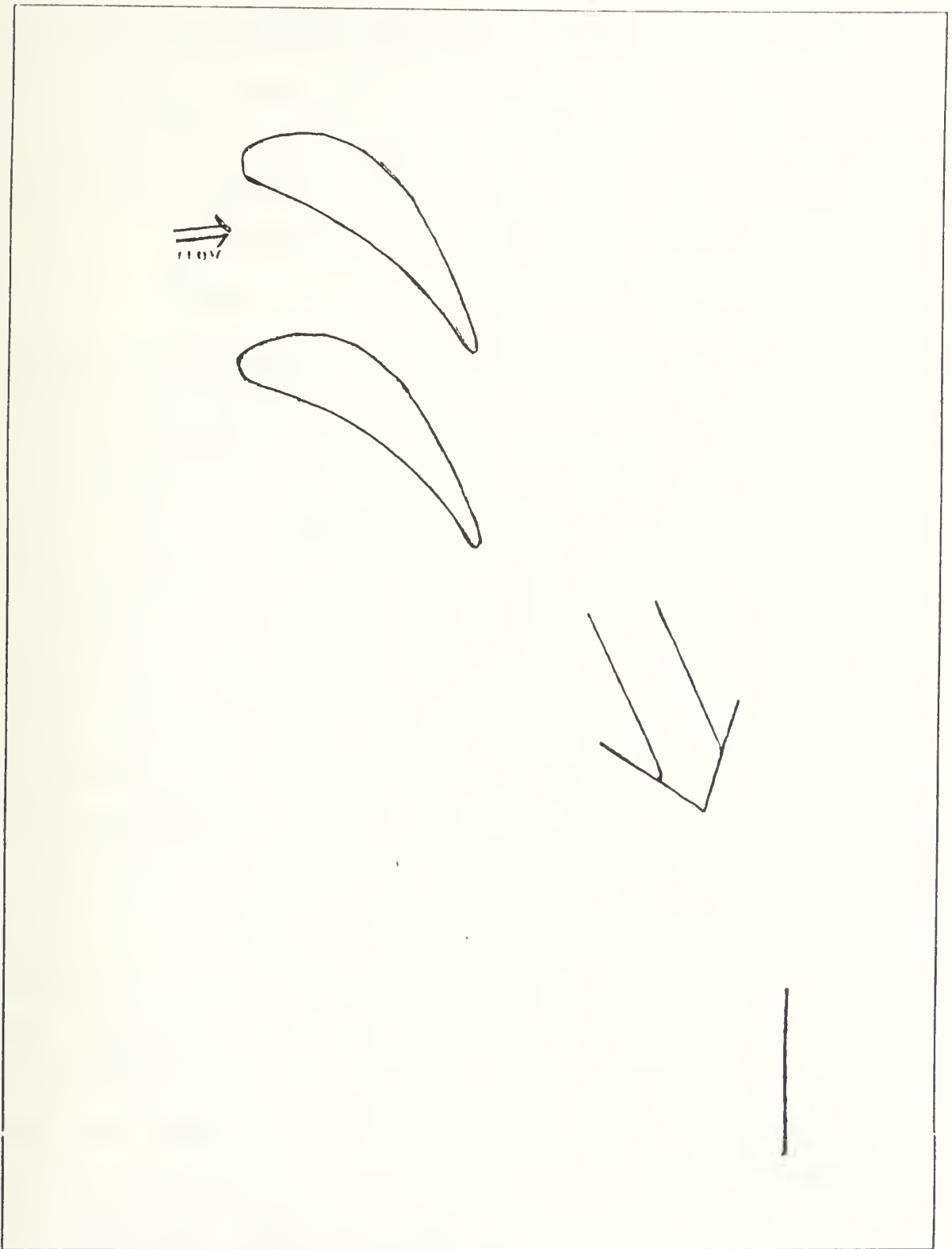


Figure 6. LDV measurement points

an angle of 50 degrees. The probe was calibrated in a free jet in which a pitot static probe was used to obtain the Mach number of the flow. This was plotted against the indicated total head, to obtain a correlation for the cobra probe. The results can be seen in Appendix C.

C. LASER SETUP

A TSI Inc. four-beam, two color fiber-optic LDV system was set up and used as a one-component system in backscatter mode. Components of the LDV optics are shown in Figure 7.

The laser was a Lexel Model 95 four-Watt argon-ion laser operating nominally at two Watts. The LDV system used four argon-ion laser beams, two blue (488 nm) and two green (514.5 nm) from a modular color separator, to measure two orthogonal velocity vectors. The color separator, and its frequency shifting Bragg cell, comprised the "Colorburst". The beams were coupled into four single-mode polarization-preserving fibers using two translator modules and two double-input couplers.

The optical fibers carried the laser power to the probe head, where the light from each fiber was collimated. The four collimated beams were focussed and crossed through a transmitting lens. Backscattered blue and green light was collected through the transmitting and receiving lenses and focused into the multimode receiving fiber. The received light from the multimode fiber was collimated with the

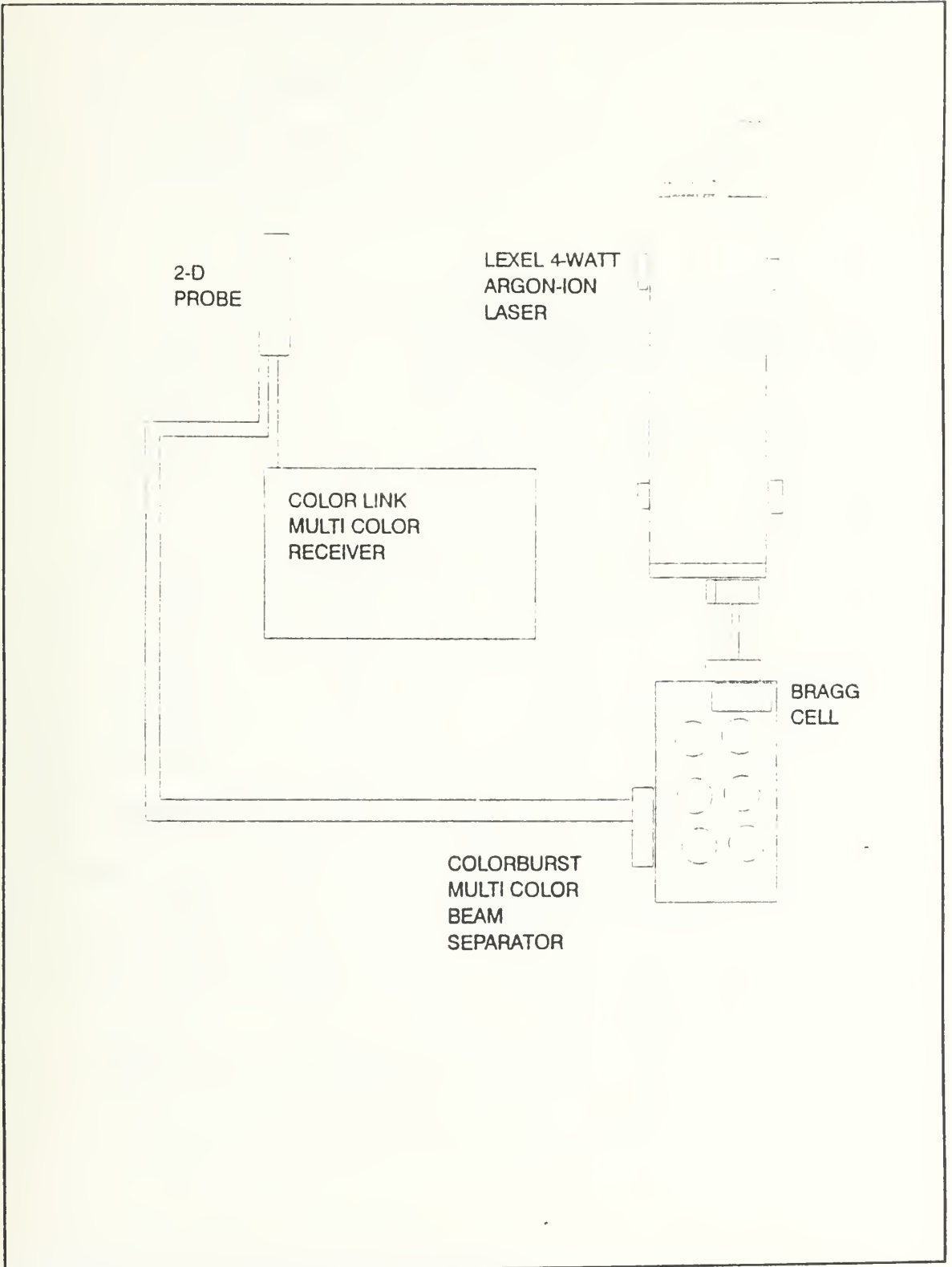


Figure 7. LDV component schematic

double-input coupler. The collimated received light was directed into a color separator to separate the light from the two velocity components. This color separator and its photomultipliers and frequency shifters comprised the "Colorlink".

LDV signals were processed by two TSI Model 1990C counter-type signal processors as shown schematically in Figure 8. The Model 1990C measured the time taken for a given number of cycles in a Doppler burst using a high resolution clock (± 1 ns).

An oscilloscope attached to the input conditioner provided real-time display of the photomultiplier output for setting filters on the counters. The counters were operated in a single measurement per burst (SM/B), coincident mode. A digital interface on the counter provided two functions. First, the master interface compared the incoming signal from each counter and checked for coincidence validation. Second, the interface provided computer input using direct memory access, sending five 16 bit words for each valid burst to the computer.

The full three-dimensional set-up and description of this system is given in Reference 5.

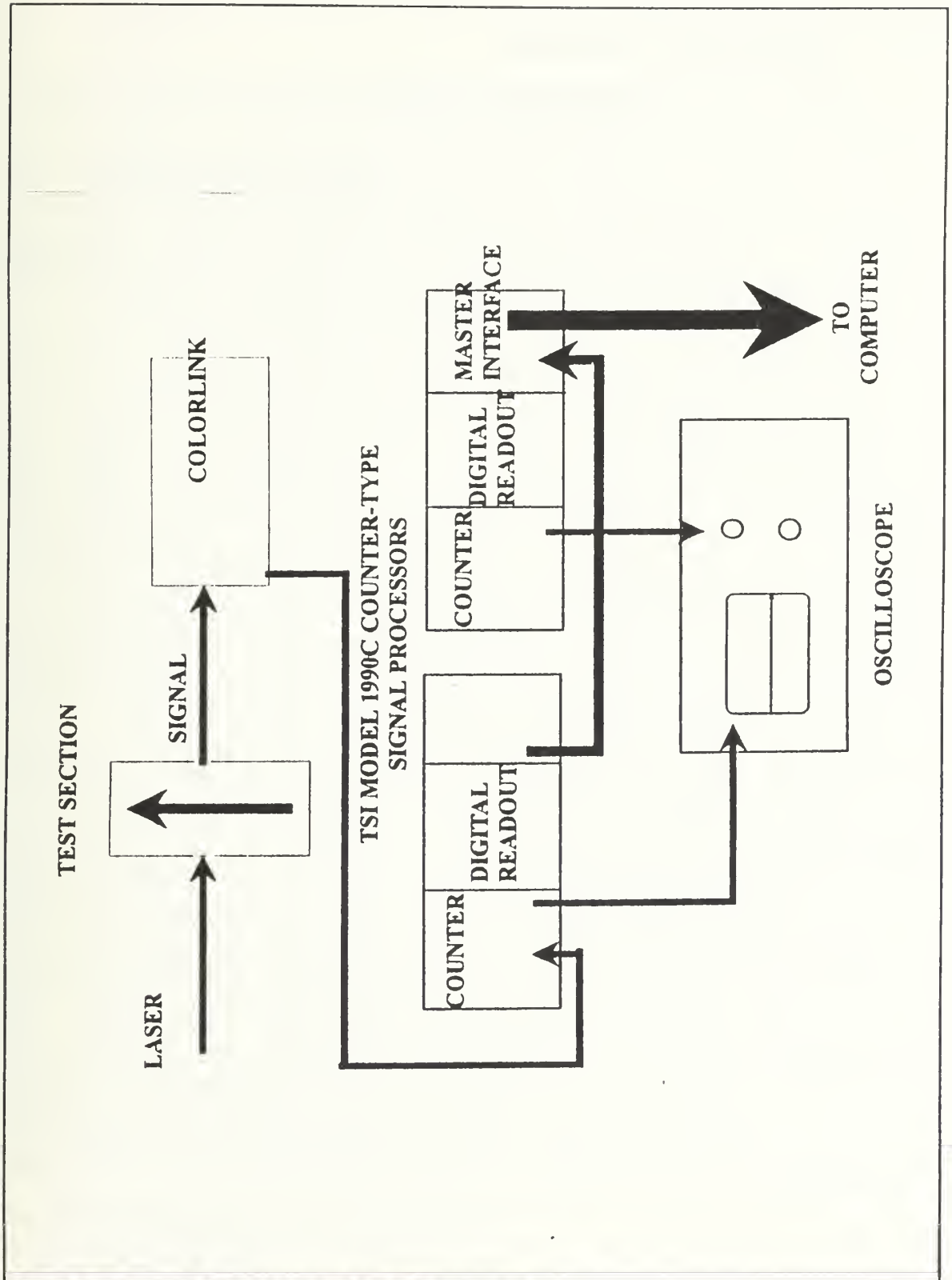


Figure 8. LDV processing hardware

D. EXPERIMENTAL PROCEDURE

When supply conditions were steady, measurements were taken during the experiment that were used as input for RVC3D. These included; upstream temperature and pressure, and downstream static pressure at the hub. These parameters were used as inputs to the computer program for the numerical simulation of the flow through the ATC.

Flowfield measurements were taken two axial chord lengths downstream from the trailing edge of the vanes, with a cobra probe. A ruler was used to position the probe when it was rotated to the next peripheral measurement location.

Initially, course surveys were performed across one blade passage. Next, finer circumferential surveys were performed across two blade wakes. This gave better resolution of the wake profiles, and also a check for flow periodicity. The initial coarse surveys, at 0.1 inch spacing were completed at 25, 50, and 75 percent span. The graphical representation of these data can be seen in Appendix C. The finer set of measurements was taken at 10, 25, 50, 75, and 90 percent span, spaced at 0.05 inches. The measurements were also extended to capture two wake regions, to check for periodicity. The tabulated data are given in Appendix C.

III. NUMERICAL SIMULATION

A. COMPUTATIONAL SCHEME

RVC3D (Rotor Viscous Code 3-D) is a computer code for the analysis of three-dimensional viscous flows in turbomachinery. The code solves the thin-layer Navier-Stokes equations with an explicit finite-difference technique. It is applicable to annular blade rows or linear cascades. Two algebraic turbulence models and a simple tip clearance model are available.

The code solves the Navier-Stokes equations formulated in a Cartesian coordinate system with rotation about the x-axis. The equations are mapped to a general body-fitted coordinate system. Streamwise viscous terms are neglected using the thin-layer assumption, but all cross-channel viscous terms are retained. Turbulence effects are modeled using either a 3-D adaptation of the Baldwin-Lomax turbulence model [Ref. 6] or the Cebeci-Smith model [Ref. 7]. The equations are discretized using second-order finite-differences and solved using a multistage Runge-Kutta scheme. References 4 and 8 describe the mathematical formulation of the RVC3D code. A sample input file for RVC3D is presented in Appendix A.

B. GRID GENERATION

The grid generation started with the schematic of the ATC, as seen in Figure 1. The drawings were digitized, to produce a set of x-y points. These data points were used as part of the input file for the GRAPE code [Ref. 9]. The input file for the GRAPE code is presented in Appendix A. This code produced a two-dimensional C-type grid about the turbine blade, as seen in Figure 9. Another FORTRAN code, STACK, takes a two-dimensional grid and stacks it into three-dimensions, using hyperbolic tangent stretching. STACK produces a grid output file that can be used by RVC3D. The namelist input for STACK is given in Appendix A. The three-dimensional grid, which has 121x31x21 grid points, can be seen in Figure 10.

A second grid generation program was also utilized. TCGRID (Turbomachinery C GRID) generates three-dimensional C- or H-type grids for turbomachinery. TCGRID generates a computational grid in a single step once the blade surfaces have been defined. The x-y coordinates, from the digitization of the drawings, were translated to z-r-theta coordinates that TCGRID could use. A FORTRAN program was written to accomplish this, and it is included in Appendix A. Once the coordinates were in the proper format they were included in the input file for TCGRID, which then produced an output file compatible with RVC3D. The input file for TCGRID is presented in Appendix A.

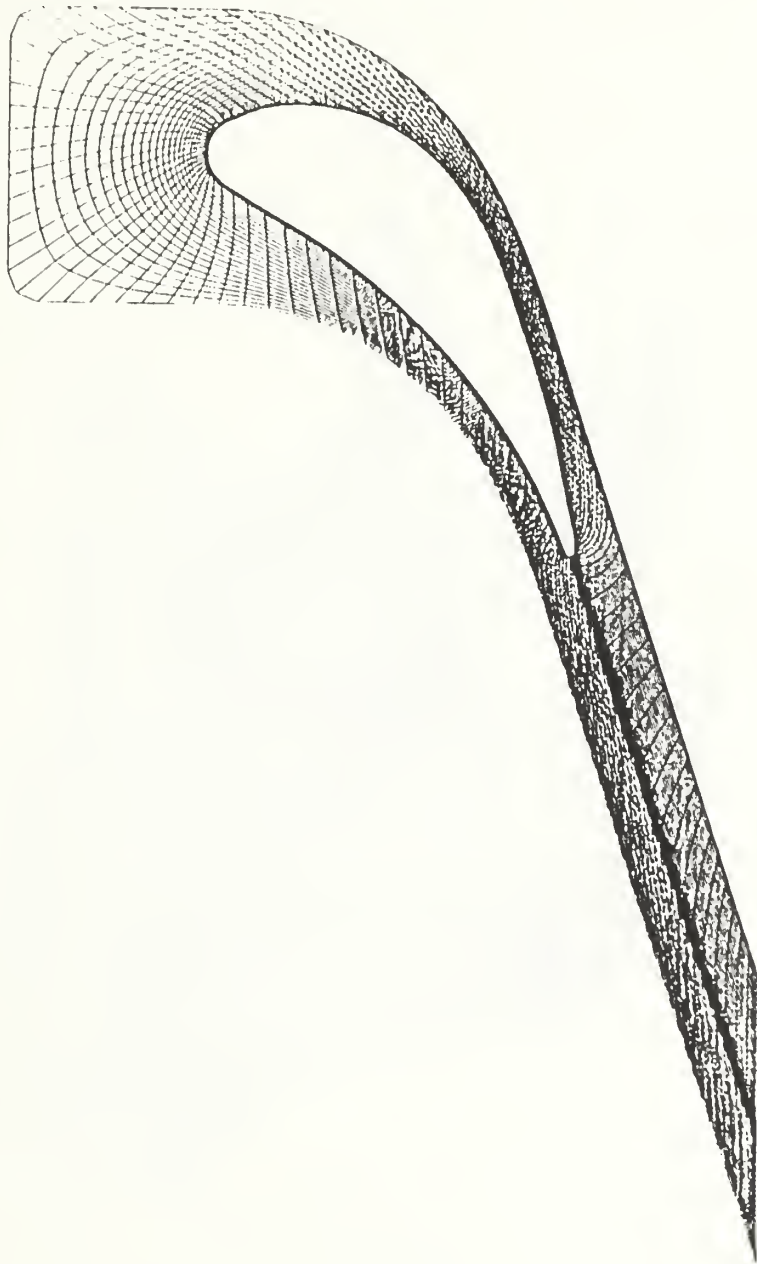


Figure 9. Grape grid

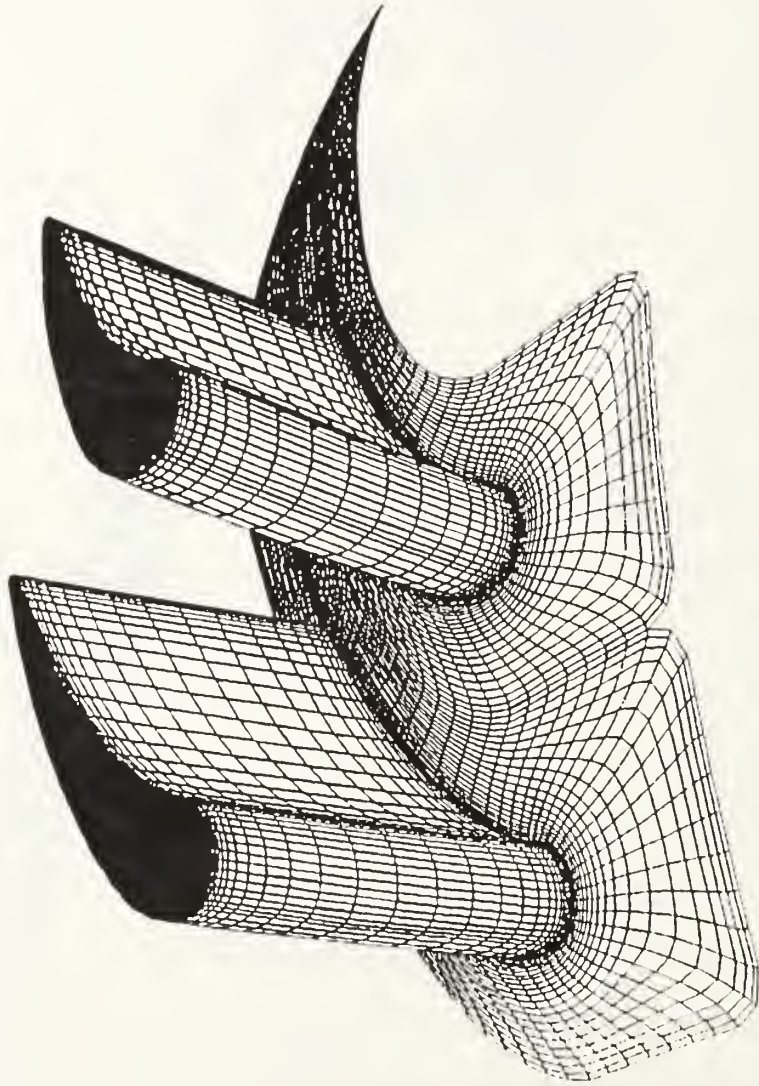


Figure 10. 3-D grid

TCGRID generates grids using the following technique:

1. A coarse, equally-spaced meridional grid is generated between the supplied hub and tip.
2. The blade geometry is interpolated onto the meridional grid.
3. 2-D blade-to-blade grids are generated along the meridional grid lines in $(m, rbar*\theta)$ coordinates, using a version of the Sorenson [9] GRAPE code.
4. The $(m, rbar*\theta)$ coordinates are transformed to (z, r, θ) .
5. The 2-D grids are reclustered spanwise to make a full 3-D grid.
6. Finally the (z, r, θ) coordinates are transformed back to (x, y, z) and written in PLOT3D format.

When the final grid was complete it was stored in a format that RVC3D could use to run the flowfield solution. After the solution was obtained, it was analyzed to ensure that it was grid independent. One way to check for grid independence is that the wake should follow the trailing edge projection and not the grid centerline.

1. GRID GENERATION COMPARISON

The grid generation programs both produced an acceptable grid. The main difference between the two was that TCGRID was a one-step process, while STACK required a GRAPE grid as an input file. It took two steps to produce a final grid using STACK, while TCGRID could produce it in one step. TCGRID also had more options available to fine-tune.

the grid. GRAPE/STACK was initially easier to use, due to prior experience with GRAPE, which allowed the first grids to be produced quickly.

TCGRID required (z,r,theta) coordinates, which were not readily available from the drawings. After data conversion, TCGRID proved very useful, and the easier of the two to manipulate.

2. RECOMMENDATIONS

If the turbine geometry data are in x-y format, the GRAPE/STACK combination is quite effective for producing early grids. These grids can be used to test the flowfield solver. GRAPE/STACK grid generation occurs in discrete steps, which helps in the process of fine-tuning the final grid. One drawback is that STACK will only stack radially.

TCGRID should be used if the turbine coordinates are given in a format that TCGRID can accept. TCGRID would also be recommended since it is a one step grid generation program that has powerful tools for manipulating the final grid. TCGRID can account for twist of the airfoil, as well as non-radial stacking and end-bends.

IV. RESULTS AND DISCUSSION

A. LASER DOPPLER VELOCIMETRY MEASUREMENTS

Three different materials were used for seeding; olive oil, water, and a glycerine oil/water mixture. The olive oil gave the best LDV signal, but contaminated the window at higher speeds. The final LDV configuration was established by directing the probe into the wake region from downstream of the cascade, as can be seen in Figure 11. Because of the current geometry of the test section only the circumferential velocity was measured. A histogram of the LDV output is given in Appendix F. The measured flow of this histogram was 76.695 M/S, at a turbulence intensity of 6.488%. At speeds higher than this, seeding became the primary problem.

B. NUMERICAL RESULTS

Figure 12 shows the computed blade surface static pressure. The figure shows results that were expected. The pressure is higher on the tip than at a corresponding point on the hub. The suction side has a steeper pressure gradient than the pressure side, and the pressures are equal at the trailing edge. Figure 13 shows the normalized blade static pressure at mid-span. The discontinuity on the suction side is due to the sonic region. Figure 14 shows

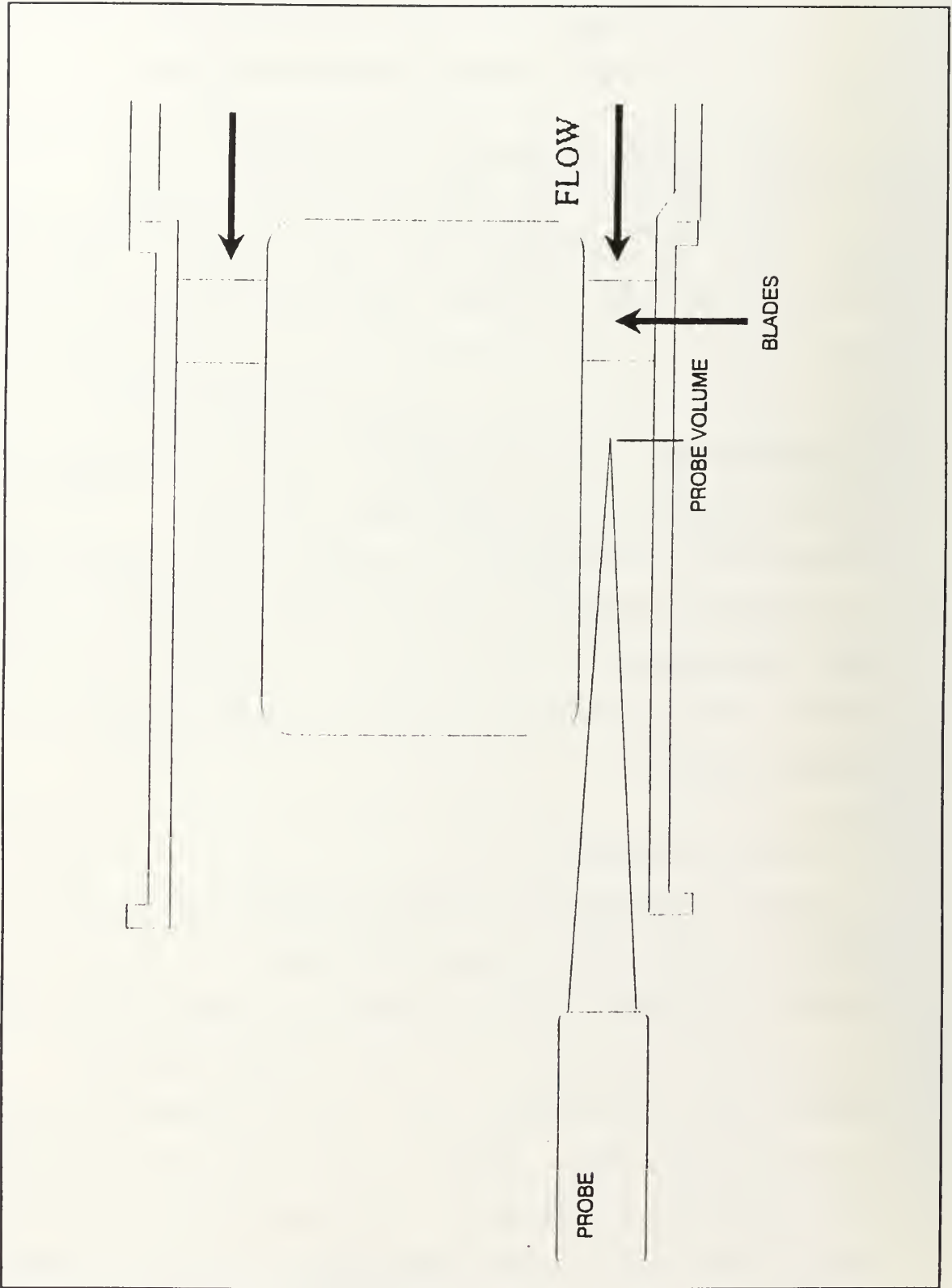


Figure 11. Probe location

PRESSURE



Figure 12. Blade surface static pressure

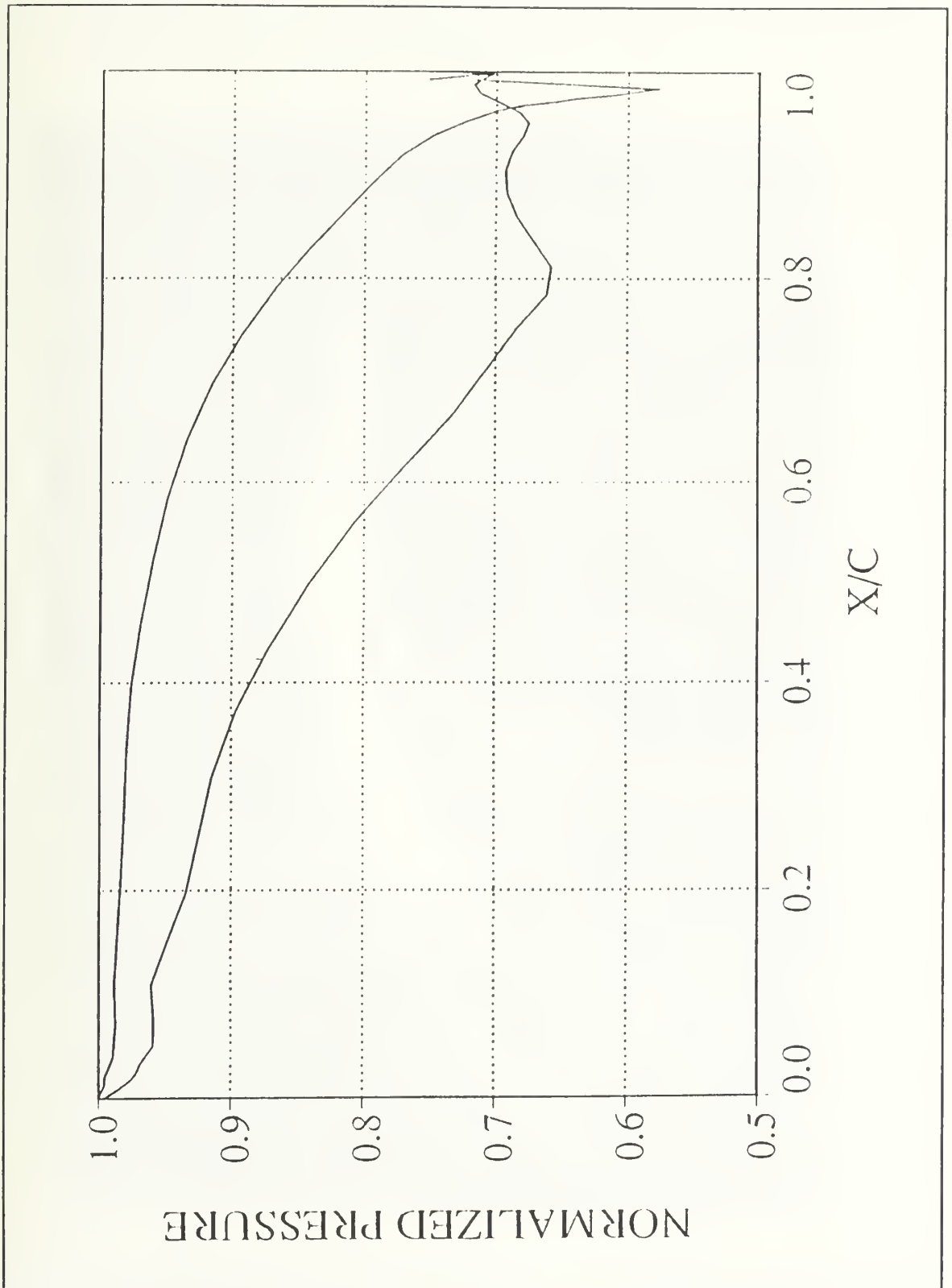


Figure 13. Blade surface static pressure at mid-span



Figure 14. Stagnation pressure on the exit plane

the stagnation pressure on a exit plane one chord length from the trailing edge. The wakes are clearly evident in this figure. Unfortunately the computational grid could not be extended two chord lengths downstream of the trailing edge. Attempts at producing larger grids gave rise to unacceptable shapes. All the flow field comparisons with the experiment were made using data computed at one chord, whereas the experimental data were measured at two chord lengths downstream.

C. COMPARISON OF DOWNSTREAM LOSSES AND EXIT FLOW ANGLES

Figure 15 is a comparison of the Mach number at 10% span predicted by the computer code, with the experimental results from the cobra probe. The velocity peak, at the 20% chord point, appears to be a jet, but upon further analysis it appears that the hub boundary layer is being pinched, and the freestream core flow is migrating toward the hub surface. This can be clearly seen in Figure 14 where the blue region is thinnest close to the hub (i.e. the core flow is migrating toward the hub endwall).

Figures 16, 17, 18, and 19 show the Mach number comparisons for flow at 25, 50, 75, and 90 percent span respectfully. The computer code does a good job predicting the wake deficit, and the width of the wake. There is good agreement at all radial locations. The core flow Mach number is about 0.65 and the jet flow in Figure 15 is only

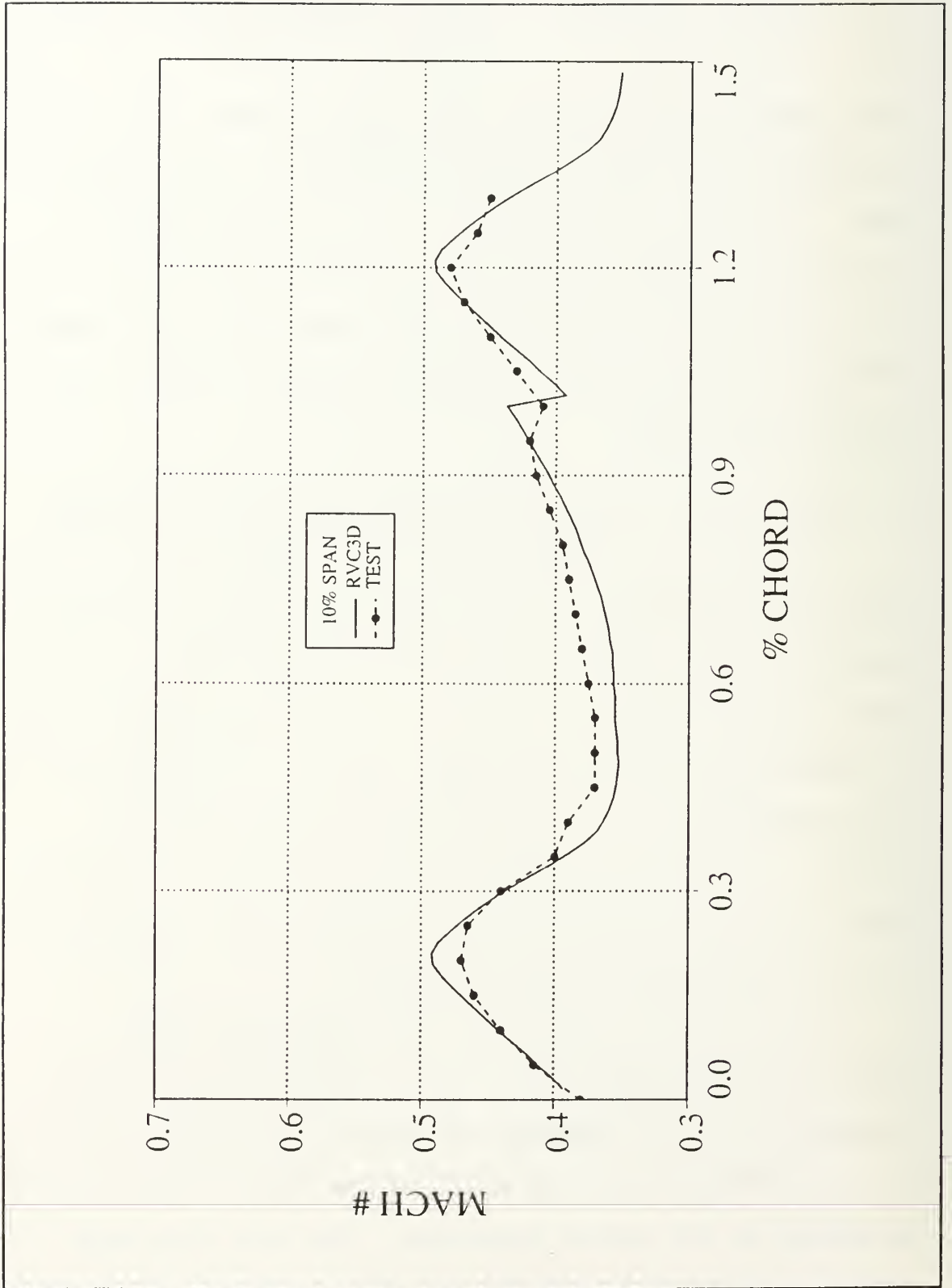


Figure 15. Mach number comparison at 10% span

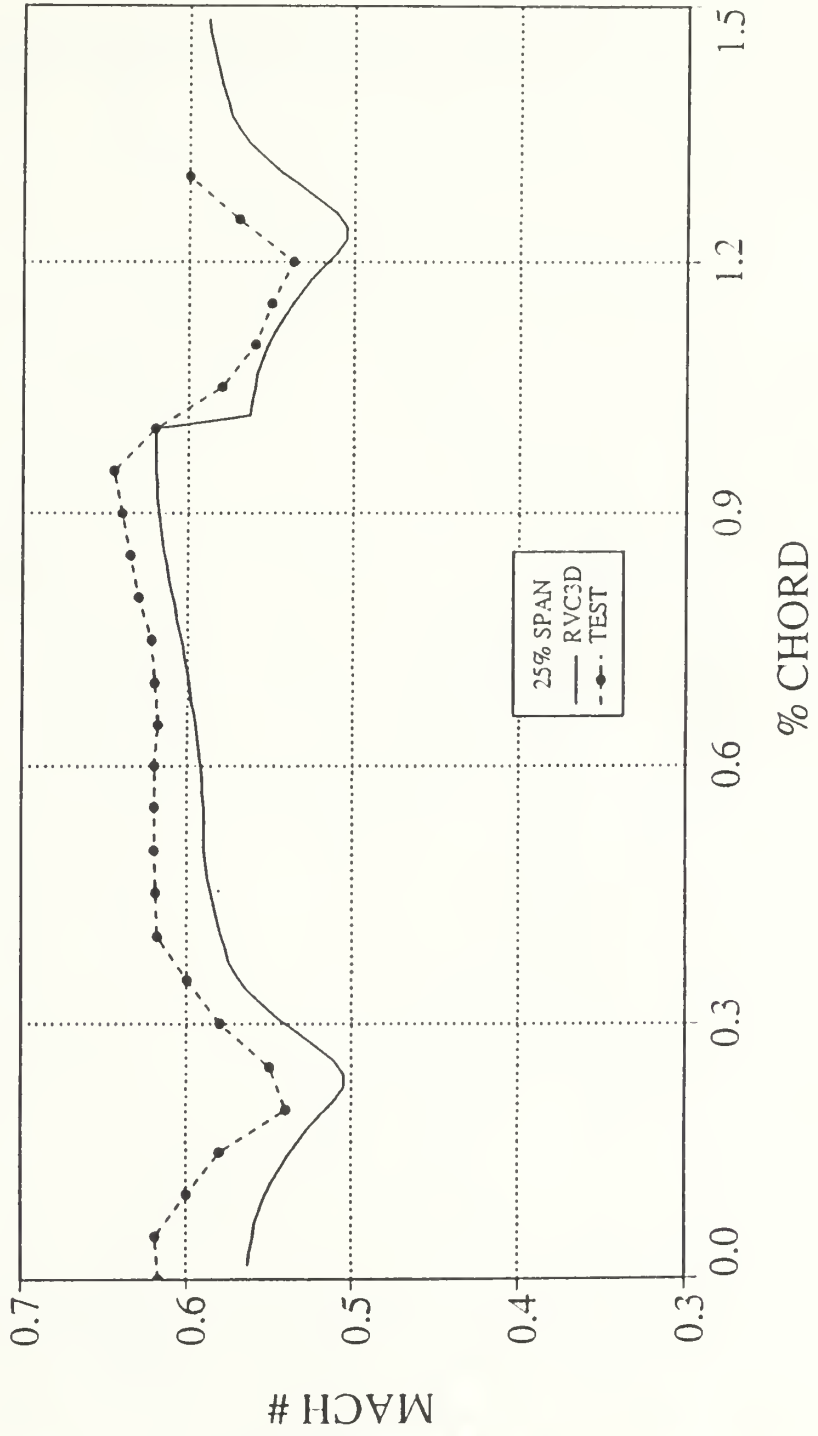


Figure 16. Mach number comparison at 25% span

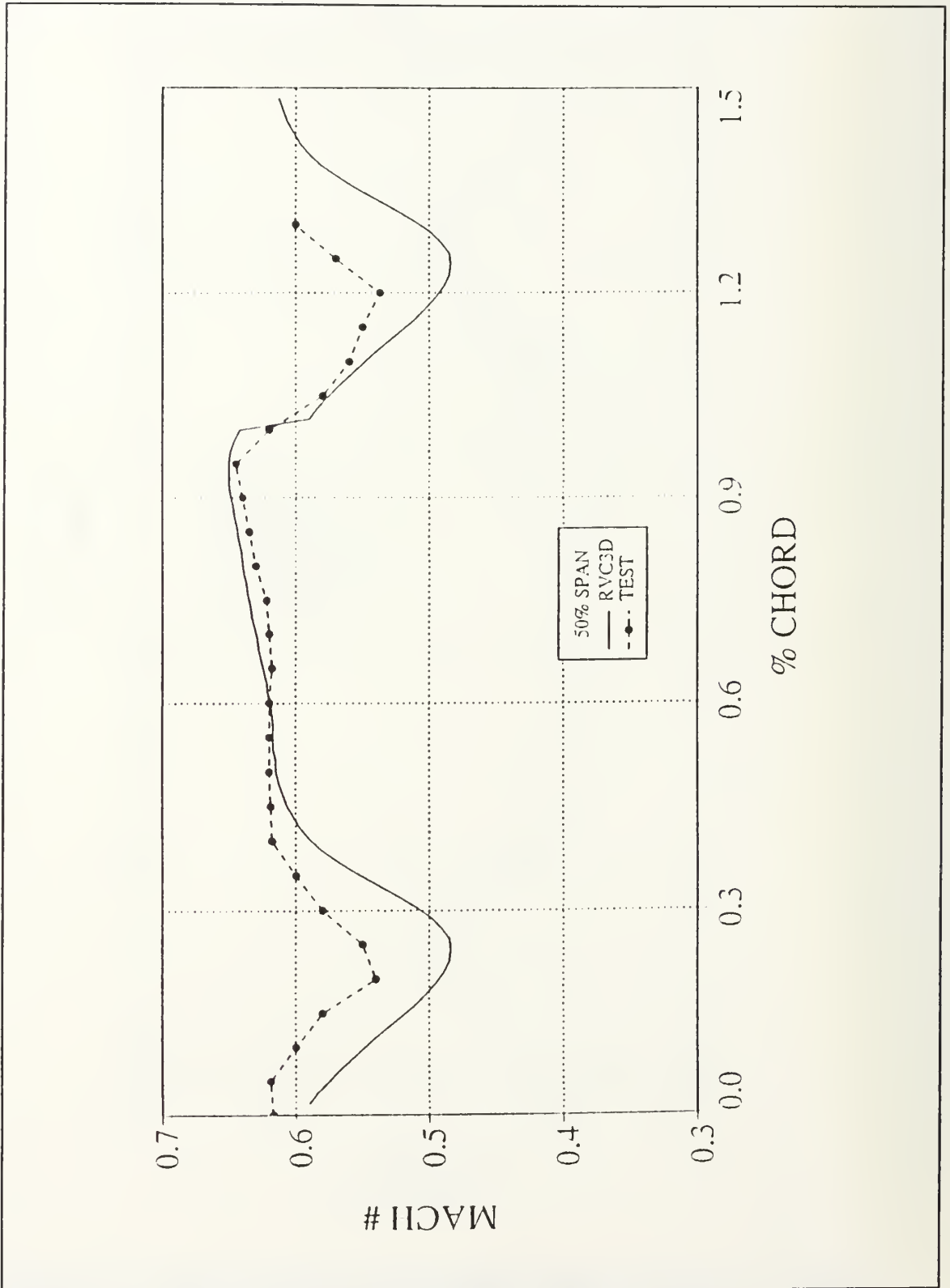


Figure 17. Mach number comparison at 50% span

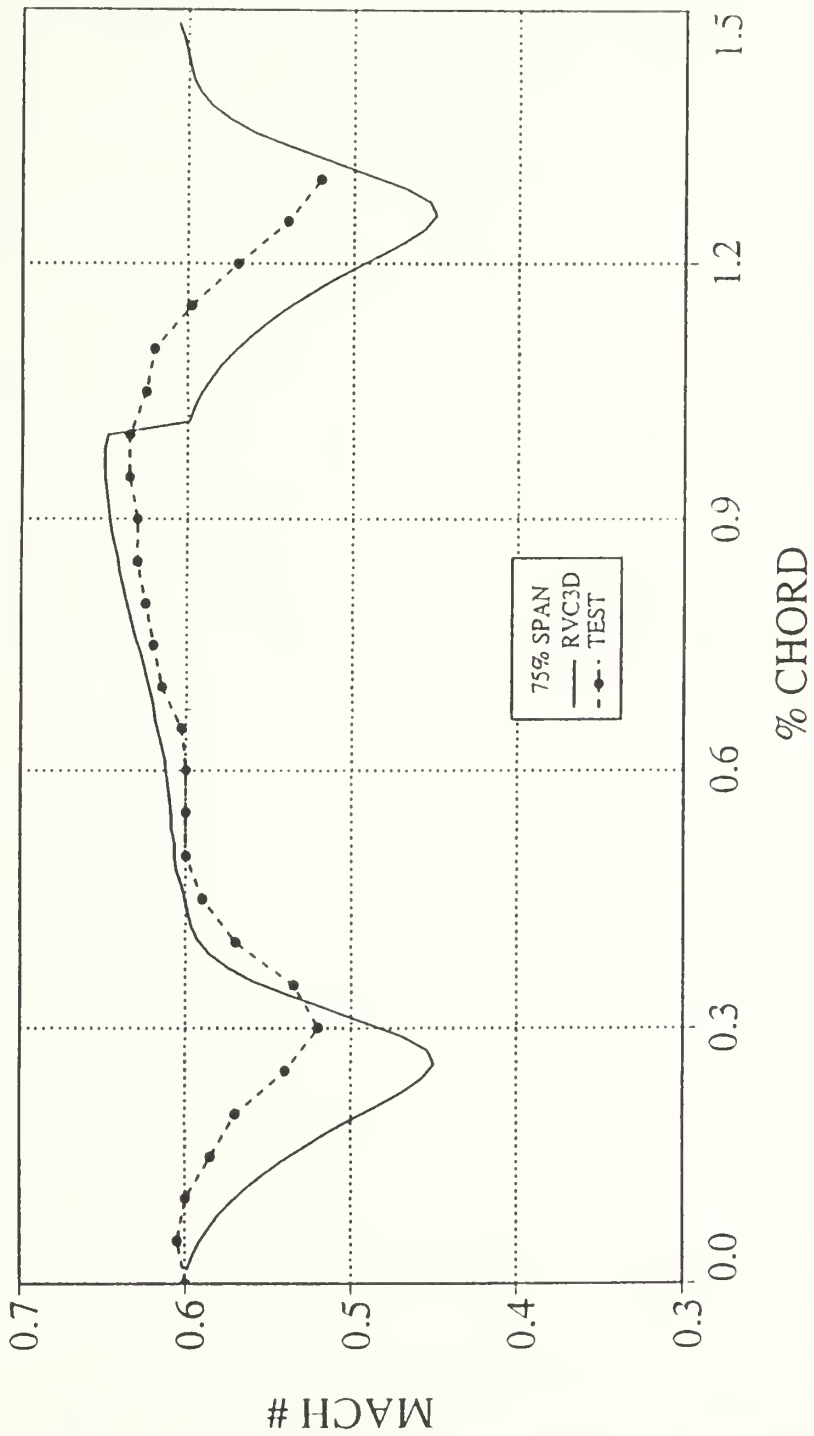


Figure 18. Mach number comparisons at 75% span

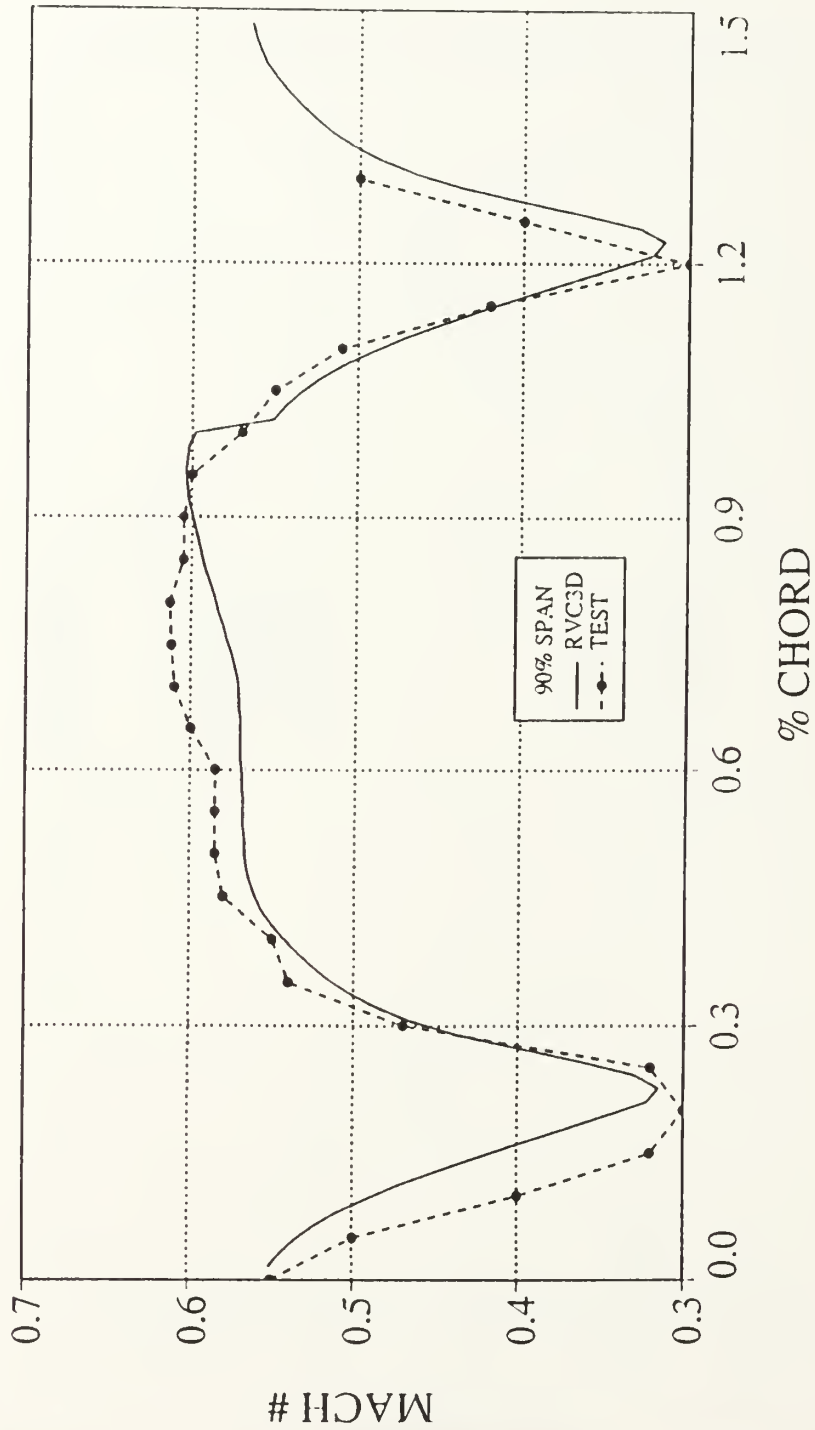


Figure 19. Mach number comparisons at 90% span

at a Mach number of 0.5. This suggests a rapid growth of the hub endwall boundary layer rather than a jet flow.

Figures 20-24 shows the flow angle comparisons for the five different radial positions that were surveyed. The overall trend in flow angle variation in the circumferential direction is predicted, but the magnitude of the flow angle is not. The computational grid may need to be reconfigured with an exit angle closer to the exit flow angle in an attempt to improve the comparison, once the axial locations of experiment and computation coincide.

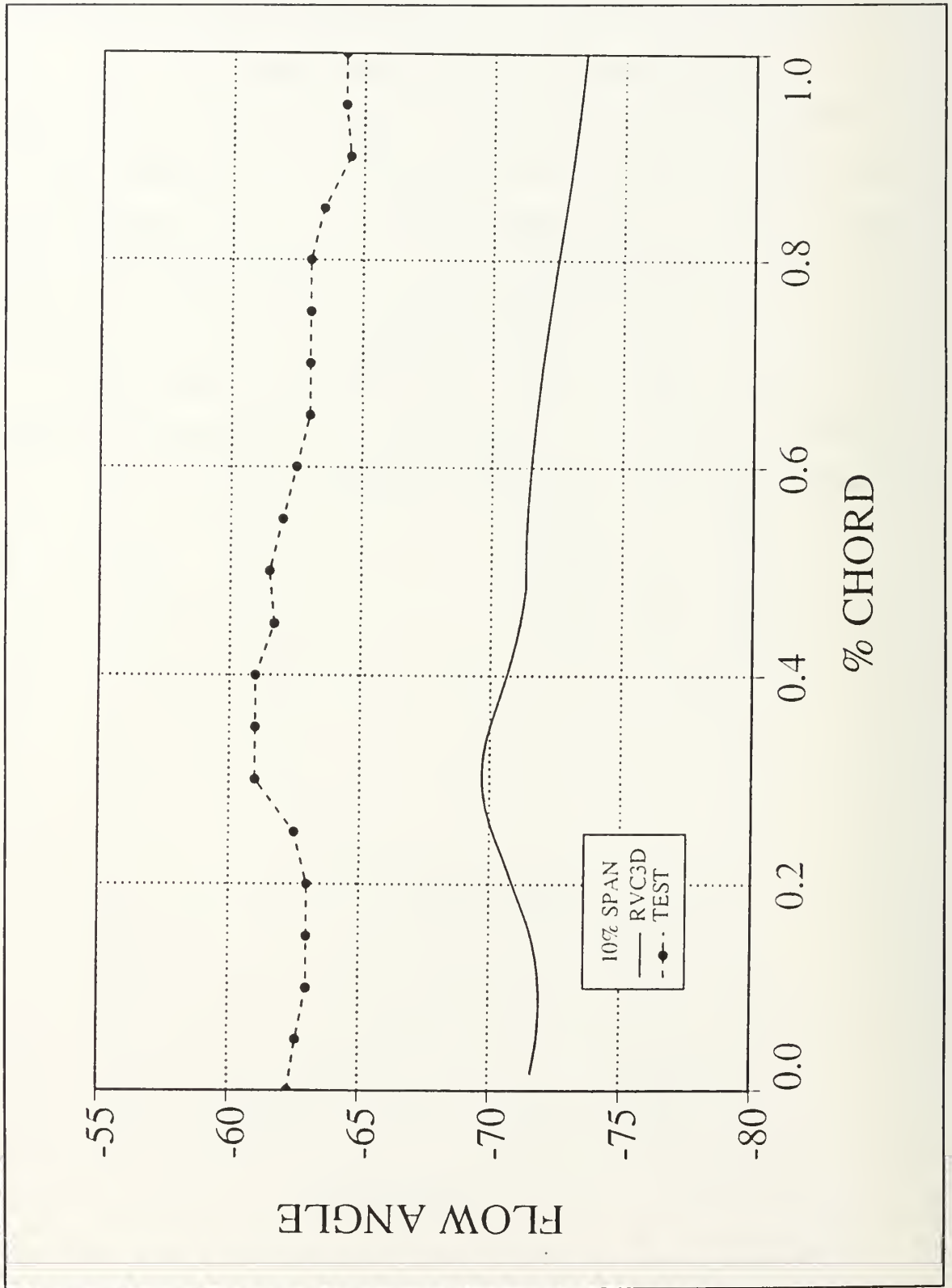


Figure 20. Flow angle comparison at 10% span

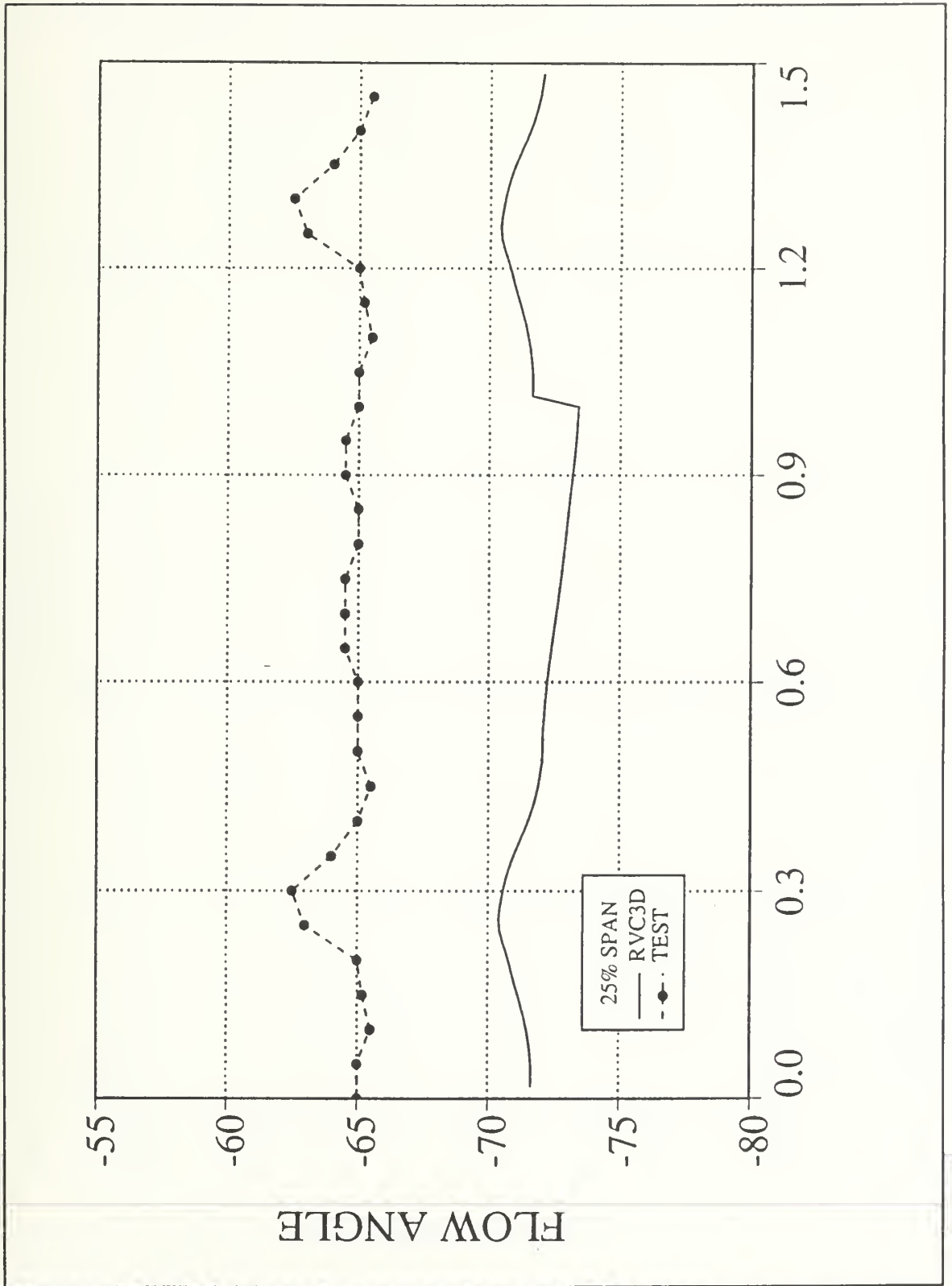


Figure 21. Flow angle comparison at 25% span

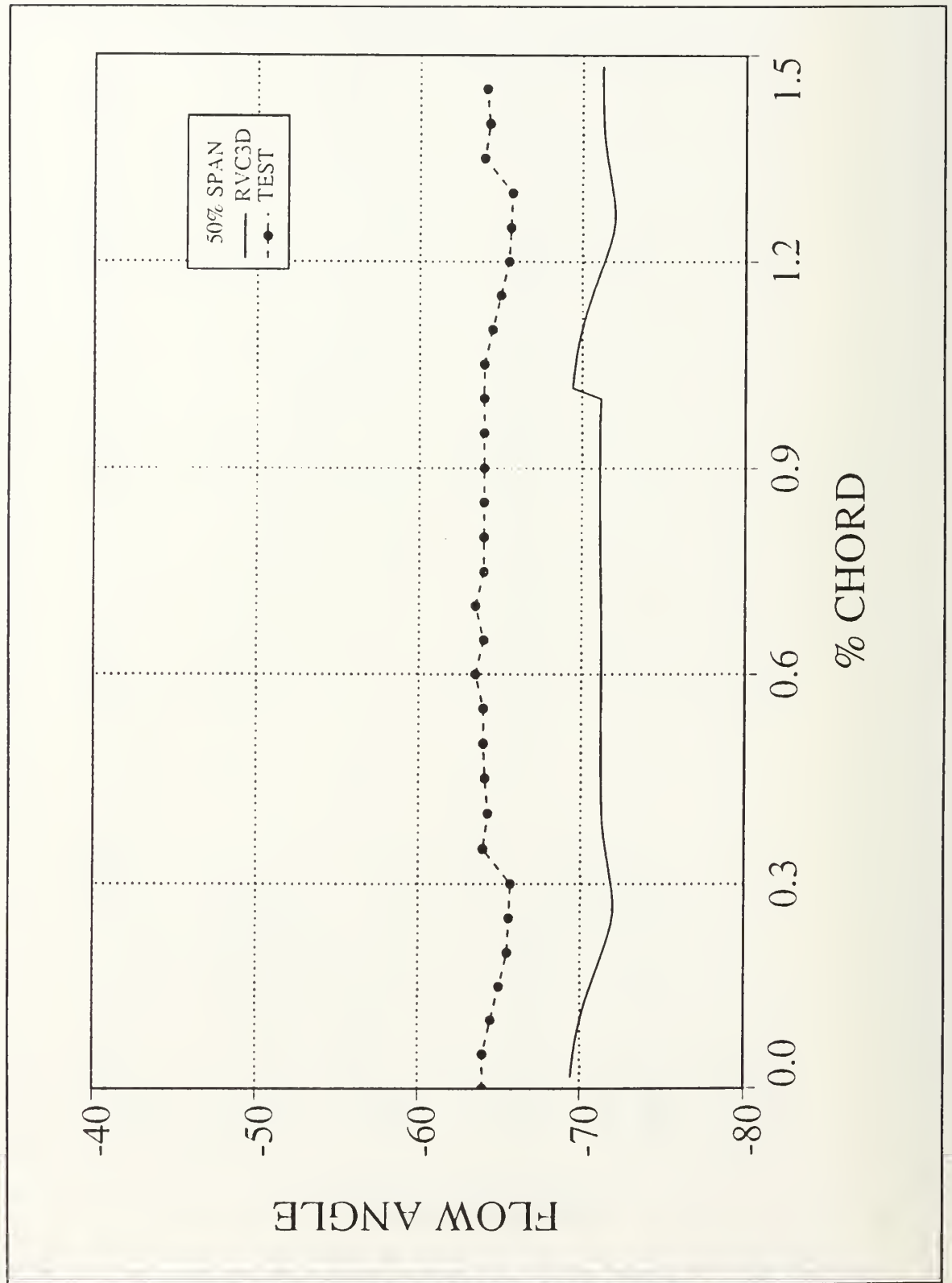


Figure 22. Flow angle comparison at 50% span

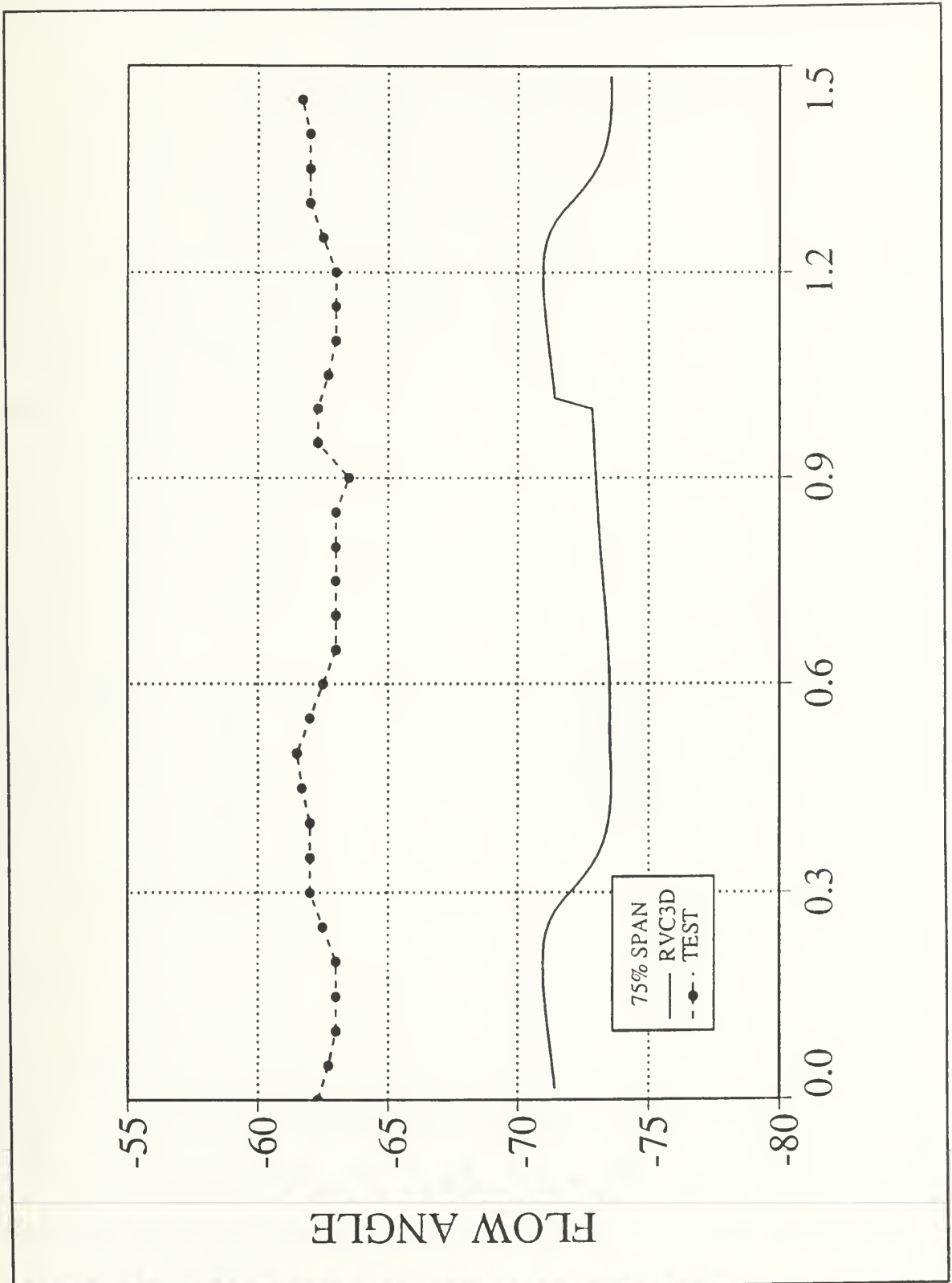


Figure 23. Flow angle comparison at 75% span

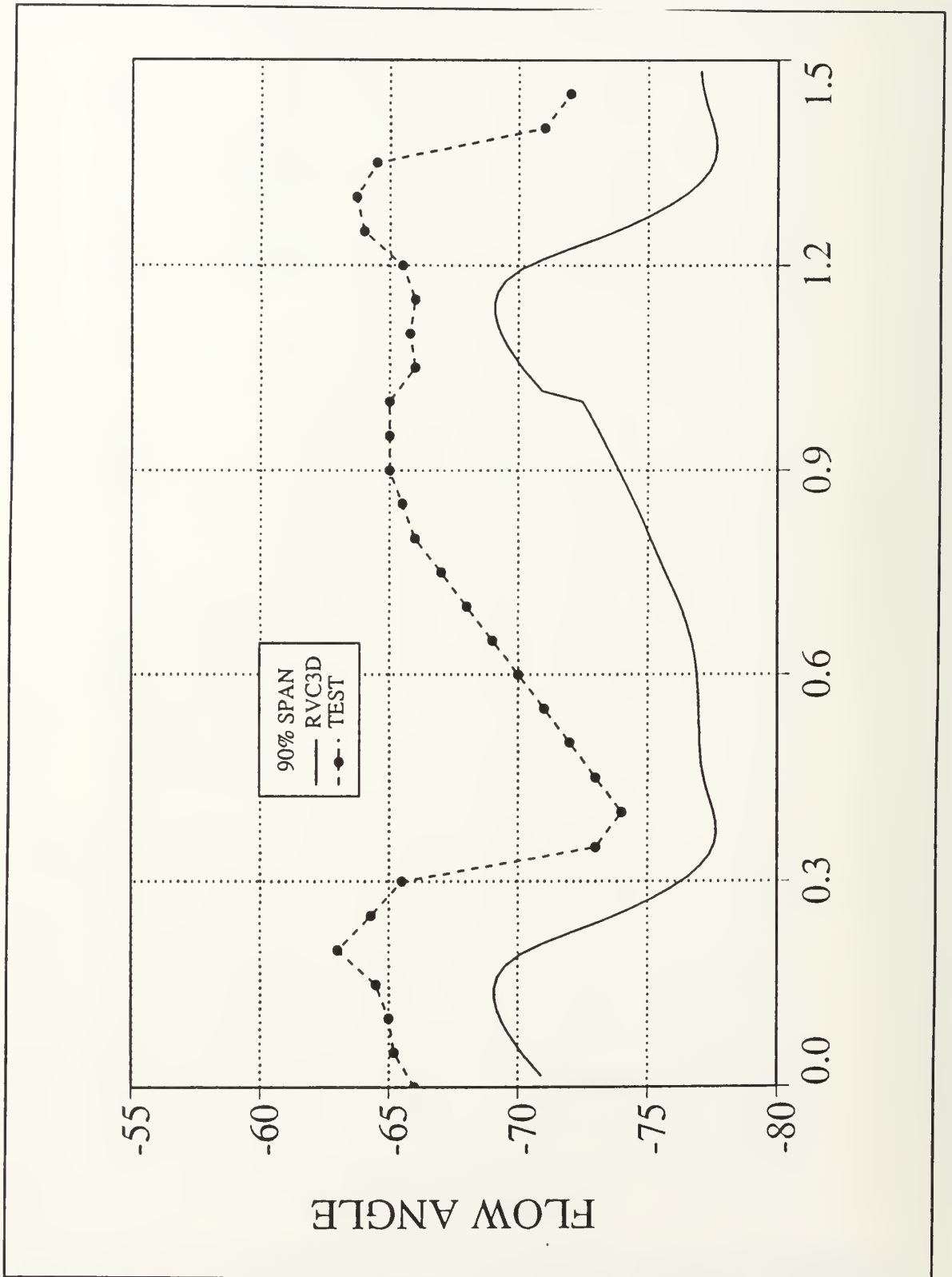


Figure 24. Flow angle comparison at 90% span

V. CONCLUSIONS AND RECOMMENDATIONS

Probe measurements were easy to take and were reliable. They allowed a quick, qualitative evaluation to be made of the computer code. The spatial resolution and accuracy were not as good as should be expected from the laser system. A further problem with the cobra probe was in the measurement of the flow angle. A hysteresis effect was evident depending on which way the probe was turned. This was compensated for by overshooting the new angle and then returning to the pneumatic balance point. The settling time on the yaw manometer was very slow due to the size of the static ports.

The computer model qualitatively predicted the measure of variation in the mean flow Mach number. The flow angle variation prediction was reasonable, given that it is a second order effect.

The computer model had run times of four hours on the Stardent, and 12 hours on the IRIS workstations. Clearly, all calculations should be done locally on the Stardent, and when resources are made available, on the Cray YMP at the National Aerodynamic Simulator.

In order to get full three-dimensional laser data, a seeding material needs to be found that will not dirty the optical access window, but will follow the streamlines.

Water evaporated before reaching the probe volume, and solids were not used due to their possible toxic nature in an enclosed facility. Olive oil was used, but the optical access window became dirty almost instantly.

The second hurdle that needs to be overcome is the glare caused by the laser beams reflecting off the hub. The reflections quickly saturate the photomultiplier, greatly reducing the signal to noise ratio. Painting the hub black helped reduce the noise significantly. Another reduction technique was to put an opaque screen between the probe and the probe volume. The screen had cutouts to allow the laser beams and the return signal clear passage, but blocked all other reflections.

A possible solution, to the glare problem, is to have the laser entering the window at a high angle so that the beams are reflected away from the optical window. This was attempted on a limited basis, but a more thorough effort needs to be undertaken. A second alternative is to attempt to get laser measurements by going back into the test cell from a downstream location. This would generate significantly less glare. The last ring of the apparatus will need to be modified to allow full optical access. Once this modification is made, measurements could be taken right up to the trailing edge. With these changes LDV data could be taken close to the endwall, and the flowfield determined in the presence of tip clearance effects.


```

3.895000 3.895000 3.895000 3.895000 3.895000 3.895000
3.895000 3.895000 3.895000 3.895000 3.895000 3.895000
3.895000 3.895000 -7.8999996E-03 -9.9200001E-03
-1.2000000E-02 -1.4080000E-02 -1.6100001E-02 -1.7999999E-02
-1.9710001E-02 -2.1190001E-03 -2.2390001E-02 -2.3280000E-02
-8.1040002E-02 -0.1503800 -0.2308900 -0.3219400 -0.4228500
-0.5328500 -0.6511000 -0.7893000 -0.9275000 -0.9410600
-0.9527700 -0.9622700 -0.9692700 -0.9735600 -0.9750000
-0.9735600 -0.9692700 -0.9622700 -0.9527700 -0.9410700
-0.9275000 -0.9124900 -0.8250000 -0.7200000 -0.6000000
-0.4560000 -0.3440000 -0.2730000 -0.2200000 -0.1820000
-0.1160000 -5.9000000E-02 -1.7000001E-02 0.0000000E+00
-1.8220000E-04 -7.2359998E-04 -1.6100000E-03 -2.8100000E-03
-4.2900001E-03 -6.0000001E-03 -7.8999996E-03 -0.1996249
-0.1997426 -0.1997819 -0.1997426 -0.1996249 -0.1994308
-0.1991690 -0.1988462 -0.1984733 -0.1980589 -0.1682508
-0.1396576 -0.1124929 -8.6961828E-02 -6.3258447E-02
-4.1563794E-02 -2.2041440E-02 -3.9694658E-03 1.4117776E-02
1.6189748E-02 1.8741548E-02 2.1701200E-02 2.4974918E-02
2.8462378E-02 3.2061070E-02 3.5659760E-02 3.9147221E-02
4.2420939E-02 4.5378406E-02 4.7932386E-02 5.0004359E-02
5.1531076E-02 5.8887679E-02 6.1068702E-02 5.7360962E-02
4.3620501E-02 2.1810250E-02 0.0000000E+00 -2.1810250E-02
-4.3620501E-02 -8.7241001E-02 -0.1308615 -0.1744820
-0.1971647 -0.1976183 -0.1980589 -0.1984733 -0.1988462
-0.1991690 -0.1994308 -0.1996249 4.585000 4.585000 4.585000
4.585000 4.585000 4.585000 4.585000 4.585000 4.585000
4.585000 4.585000 4.585000 4.585000 4.585000 4.585000
4.585000 4.585000 4.585000 4.585000 4.585000 4.585000
4.585000 4.585000 4.585000 4.585000 4.585000 4.585000
4.585000 4.585000 4.585000 4.585000 4.585000 4.585000
4.585000 4.585000 4.585000 4.585000 4.585000 4.585000
4.585000 4.585000 4.585000 4.585000 4.585000 4.585000

```

This is the input for RVC3D:

```

'TRANSONIC TURBINE Annular Cascade'
&n11 im=121 jm=31 km=21 itl=21 iil=54 &end
&n12 cfl=5.5 avisc1=0.0 avisc2=0.0 avisc4=0.30 ivdt=1
    nstg=4 itmax=1100 irs=1 epi=0.50 epj=0.60 epk=0.60
    &end
&n13 ibcin=3 ibcex=3 isymt=0 ires=10 icrnt=50
    iresti=0 iresto=1 ibcpw=0 iqin=0 &end
&n14 emxx=0.13 emty=0.0 emrz=0.0 expt=0.0 prat=0.6800
    ga=1.4 om=0.000000 igeom=1 alex=-67.0 &end
&n15 ilt=3 tw=1.00 renr=5.000e5 prnr=.7 prtr=.9
    vispwr=.666666 srtip=0.0 cmutm=14. jedge=15 kedge=11
    iltin=2 dblh=0.0024 dblt=0.0089 &end
&n16 io1=1 io2=165 oar=0. ixjb=0 njo=1 nko=3
    jo=1 ko=5 11 16 &end

```

This is the input file to GRAPE, for the Annular Turbine Cascade :

```
&GRID1 jmax=121,kmax=21,ntetyp=3,nairf=5,jairf=51,nibdst=7,
jtebot=40,jtetop=121,nobshp=7,xleft=-1.5,xle=-.975,
xte=0.0,xright=.75,rcorn=.08,dsi=.001,norda=4,3,
maxita=200,400,nout=4 &end
&GRID2 dsra=.45,pitch=.7895 &end
&GRID3
  airfx=-.0079000,-.0099200,-.0120000,-.0140800,-.0161000,
-.0180000,-.0197100,-.0211900,-.0223900,-.0232800,-.0810400,
-.1503800,-.2308900,-.3219400,-.4228500,-.5328500,-.6511000,
-.7893000,-.9275000,-.9410600,-.9527700,-.9622700,-.9692700,
-.9735600,-.9750000,-.9735600,-.9692700,-.9622700,-.9527700,
-.9410700,-.9275000,-.9124900,-.8250000,-.7200000,-.6000000,
-.4560000,-.3440000,-.2730000,-.2200000,-.1820000,-.1160000,
-.0590000,-.0170000,0.0000000,-.0001822,-.0007236,-.0016100,
-.0028100,-.0042900,-.00600000,-.0079000,
  airfy=-.9152800,-.9158200,-.9160000,-.9158200,-.9152800,
-.9143900,-.9131900,-.9117100,-.9100000,-.9081000,-.7714300,
-.6403300,-.5157800,-.3987200,-.2900400,-.1905700,-.1010600,
-.0182000,0.0647300,0.0742300,0.0859300,0.0995000,0.1145100,
0.1305000,0.1470000,0.1635000,0.1794900,0.1945000,0.2080600,
0.2197700,0.2292700,0.2362700,0.2700000,0.2800000,0.2630000,
0.2000000,0.1000000,0.0000000,-.1000000,-.2000000,-.4000000,
-.6000000,-.8000000,-.9040000,-.9060800,-.9081000,-.9100000,
-.9117100,-.9131900,-.9143900,-.9152800,
&end
```

This is the namelist for STACK:

```
&n11 km=21 rhub=3.895 rtip=4.585 nblade=31 ysp=-.3 dh1=0.01
dt1=0.01 &end
```

This program outputs the velocity and flow angle on the exit plane. This is read from the Q file.

```

C*****
*****
c    plane.f reads rvc3d files & writes ascii files for
xyplot
c    unit 1 = input xyz file
c    unit 3 = input q file
c    unit 7 = output exit velocities on 5 k-planes
c    unit 8 = output flow angles on 5 k-planes
c    unit 4 = output residual history
C*****
*****
        parameter(ni=121,nj=31,nk=21)
        real x(ni,nj,nk),y(ni,nj,nk),z(ni,nj,nk)
        real qq(5,ni,nj,nk),resd(5000,5)
        dimension kk(5),v(5),ang(5)
c    k-values are hard-wired below
        data kk/4,7,11,15,18/
C*****
*****
c    read grid coordinates
C*****
*****
        read(1,*)im,jm,km
        read(1,*)((x(i,j,k),i=1,im),j=1,jm),k=1,km),
1          ((y(i,j,k),i=1,im),j=1,jm),k=1,km),
2          ((z(i,j,k),i=1,im),j=1,jm),k=1,km)
C*****
*****
c    read restartT file
C*****
*****
        read(3,*)imax,jmax,kmax
        read(3,*)fsmach,alpha,re,time
c
        icode=iabs(im-imax)+iabs(jm-jmax)+iabs(km-kmax)
        if(icode.ne.0)then
        write(6,610)im,jm,km,imax,jmax,kmax
        stop
        endif
c
read(3,*)((qq(l,i,j,k),i=1,im),j=1,jm),k=1,km),l=1,5)
c
c    additional residual data
        read(3,*)itl,iil,phdeg,ga,om,nres,dum,dum,dum,dum
        read(3,*)((resd(nr,l),nr=1,nres),l=1,5)
C*****
*****

```

```

*****
c      velocities and flow angles to unit 7 and 8
c*****
*****
      k=kk(3)
      i=1
      do 10 j=jmax,1,-1
      um=um+1
      do 15 l=1,5
      k=kk(1)
      rho=qq(1,i,j,k)
      v(l)=((qq(2,i,j,k)/rho)**2+(qq(3,i,j,k)/rho)**2)**.5
      ang(l)=atan(qq(3,i,j,k)/qq(2,i,j,k))*57.3
15 continue
      umper=um/62
      write(7,300)umper,(v(l),l=1,5)
      write(8,300)umper,(ang(l),l=1,5)
10 continue
      i=121
      do 30 j=1,jmax,1
      um=um+1
      do 25 l=1,5
      k=kk(1)
      rho=qq(1,i,j,k)
      v(l)=((qq(2,i,j,k)/rho)**2+(qq(3,i,j,k)/rho)**2)**.5
      ang(l)=atan(qq(3,i,j,k)/qq(2,i,j,k))*57.3
25 continue
      umper=um/62
      write(7,300)umper,(v(l),l=1,5)
      write(8,300)umper,(ang(l),l=1,5)
30 continue
c*****
*****
c      residual history output to unit 4
c*****
*****
      write(4,310) 1,(resd(1,l),l=1,5)
      do 40 j=2,nres
      it=10*(j-1)
40 write(4,310)it,(resd(j,l),l=1,5)
c*****
*****
300 format(6f8.3)
310 format(i5,5(1x,e10.3))
610 format(' ***** warning *****',/,
1      ' im, jm, km, read from input',3i5,' do not
match',/,
2      ' im, jm, km, read from restart file',3i5)
      stop
      end

```

This program converts the x,y data point into r,z,theta coordinates for TCGRID:

```
dimension x(5),y(5),r(5)
data r/3.941,4.033,4.240,4.446,4.539/
do 10 theta=-.105,.105,.014
do 20 l=1,5
rad=r(l)
y(l)=(rad*sin(theta))*25.4
x(l)=(rad*cos(theta)-3.895)*25.4
20 continue
write(9,100) (x(l),y(l),l=1,5)
10 continue
100 format(10f7.3)
stop
end
```

APPENDIX B. RVC3D USER'S GUIDE

INTRODUCTION

RVC3D is a computer code for analysis of three-dimensional viscous flows in turbomachinery. Some printed output is available, but graphics software will be needed for examining the solution files. Restart files are in the standard qfile format for the **plot3d** or **fast** graphic codes developed at NASA Ames Research Center.

C-type grids are used to give good resolution of blade leading-edges and wakes. Grid input is in standard **plot3d** xyz-file format, so any C-grid generator can be used. However two grid codes have been developed specifically for use with **rvc3d**: **stack** and **tcgrid**. **STACK** reads a 2-D grid generated by the **grape** code, and generates a 3D grid for a linear or annular blade row by stacking the 2-D grid spanwise. **tcgrid** is a general 3-D C- or H-grid generator for turbomachinery. It reads annulus and blade geometry in either **meridl** format or NASA Lewis compressor design code format. It generates C-type grids at several spanwise locations using a version of the **grape** code, then reclusters the grids spanwise.

STARDENT SETUP AND EXECUTION

Parameter statements are used to make redimensioning simple. The **parameter** statement is located throughout the code and must be modified to the dimensions of the input grid. Using a **vi** editor, this can be accomplished by typing the following command at the editor prompt:

```
:1,$ s/ni=old,nj=old,nk=old/ni=new,nj=new,nk=new/g
```

the **j** component must be one greater than the **j** dimension of the grid.

After the parameter statement is changed the code must be recompiled, with the following statement:

```
>fc -O3 rvc3d.f -o rvc3d
```

The input file for **rvc3d** must also be modified to set up for the flow conditions. The steps for this can be found in the program documentation.

Rvc3d is run as a standard unix process:

```
>rvc3d < input > output
```

It is recommended that this input be put in a **.com** file and then submitted as a batch job. For example:

```
>batch < rvc3d.com
```


APPENDIX C. COBRA PROBE MEASUREMENTS

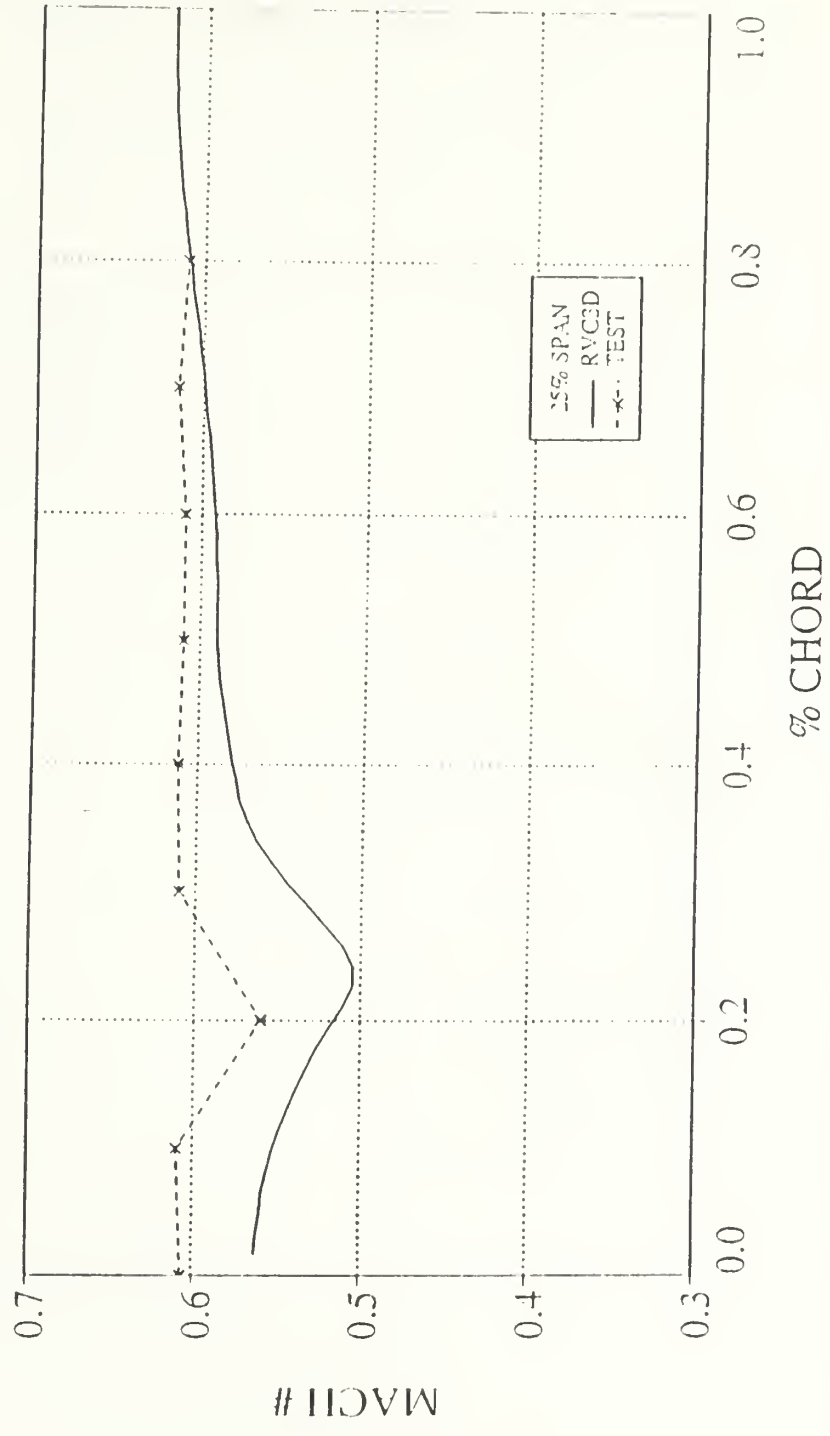
This table shows the mach numbers obtained by the cobra probe at various span locations.

% CHORD	10%	25%	50%	75%	90%
0.0	.38	.607	.617	.60	.55
0.05	.415	.608	.619	.605	.50
0.1	.41	.61	.60	.60	.49
0.15	.46	.58	.58	.585	.32
0.2	.47	.56	.54	.57	.39
0.25	.45	.565	.55	.51	.32
0.3	.44	.61	.58	.52	.17
0.35	.40	.611	.60	.535	.51
0.4	.39	.612	.618	.57	.55
0.45	.37	.611	.619	.59	.58
0.5	.37	.61	.62	.60	.585
0.55	.37	.615	.62	.60	.585
0.6	.375	.61	.62	.60	.585
0.65	.38	.612	.618	.603	.60
0.7	.385	.615	.62	.615	.61
0.75	.39	.612	.622	.62	.612
0.8	.395	.61	.63	.625	.613
0.85	.405	.61	.635	.63	.605
0.9	.415	.612	.64	.63	.605
0.95	.42	.613	.615	.635	.60
1.00	.41	.607	.62	.635	.57
1.05	.43	.608	.58	.625	.55
1.1	.45	.61	.56	.62	.51
1.15	.47	.58	.55	.598	.42
1.2	.48	.56	.537	.57	.30
1.25	.46	.565	.57	.54	.40
1.3	.45	.61	.60	.52	.50

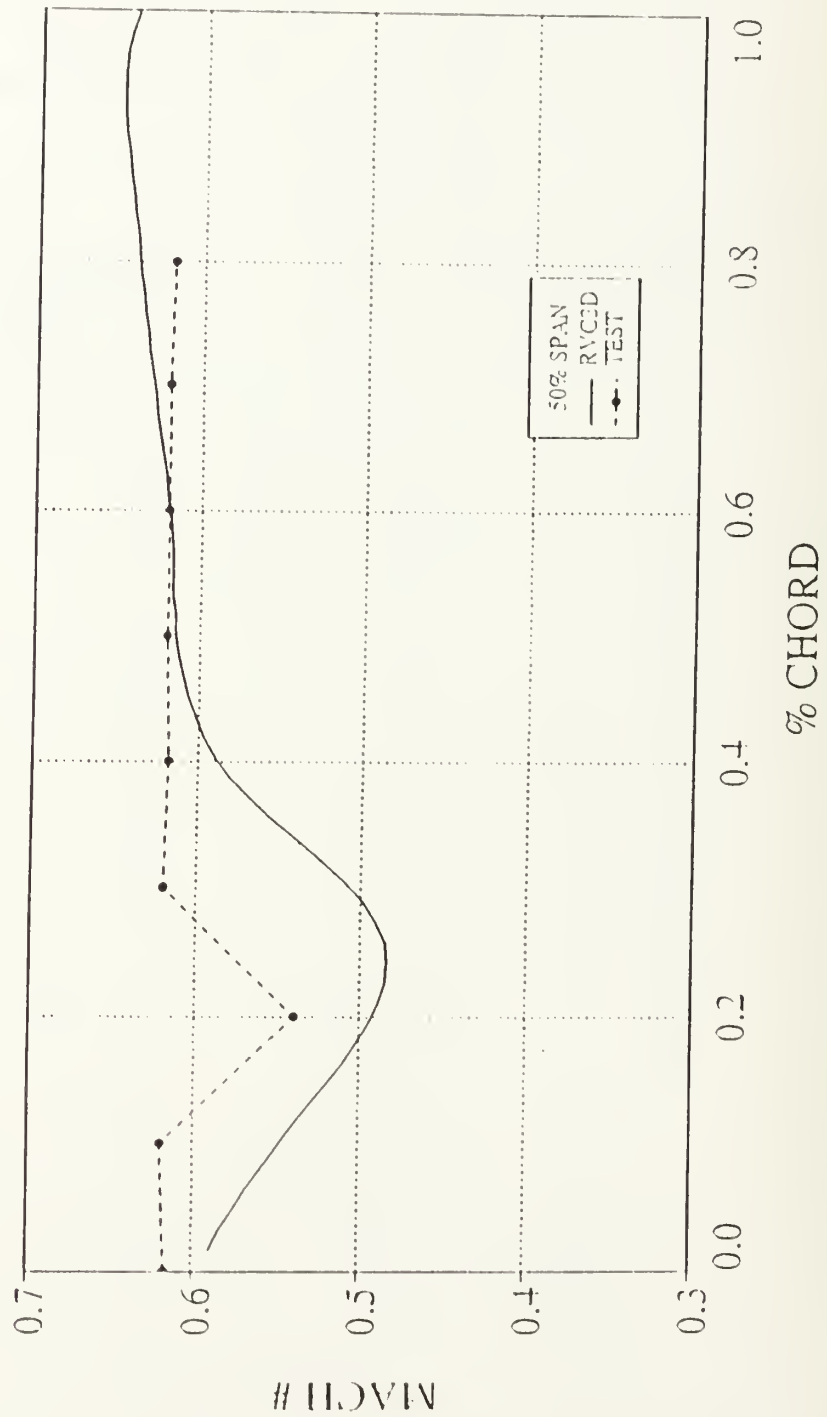
This table shows the flow angles as measured by the cobra probe.

% CHORD	10%	25%	50%	75%	90%
0.0	62	65	62	62.5	66
0.05	62.5	65	63	63	65
0.1	63	65.5	63	63	65
0.15	63	65	63	63	64.5
0.2	62.5	65	63	62.5	63
0.25	61	63	62.5	62	64.5
0.3	61	62.5	62	62	65.5
0.35	61	64	62	62	73
0.4	61	65	62	62	74
0.45	61.5	65.5	62	62	73
0.5	61.5	65	61.5	61.5	72
0.55	62	65	62	62	71
0.6	62.5	65	62.5	62.5	70
0.65	63	64.5	63	63	69
0.7	63	64.5	63	63	68
0.75	63	64.5	63	63	67
0.8	63	65	63	63	66
0.85	63.5	65	63.5	63	65.5
0.9	64.5	64.5	64.5	63.5	65
0.95	64.5	64.5	64	62.5	65
1.00	64.5	65	64	62.5	65
1.05	63	65	63	63	66
1.1	63	65.5	63	63	65.8
1.15	63	65	63	63	66
1.2	63	65	63	63	65.5
1.25	62.5	63	62.5	62.5	65.5
1.3	62	62.5	62	62	64

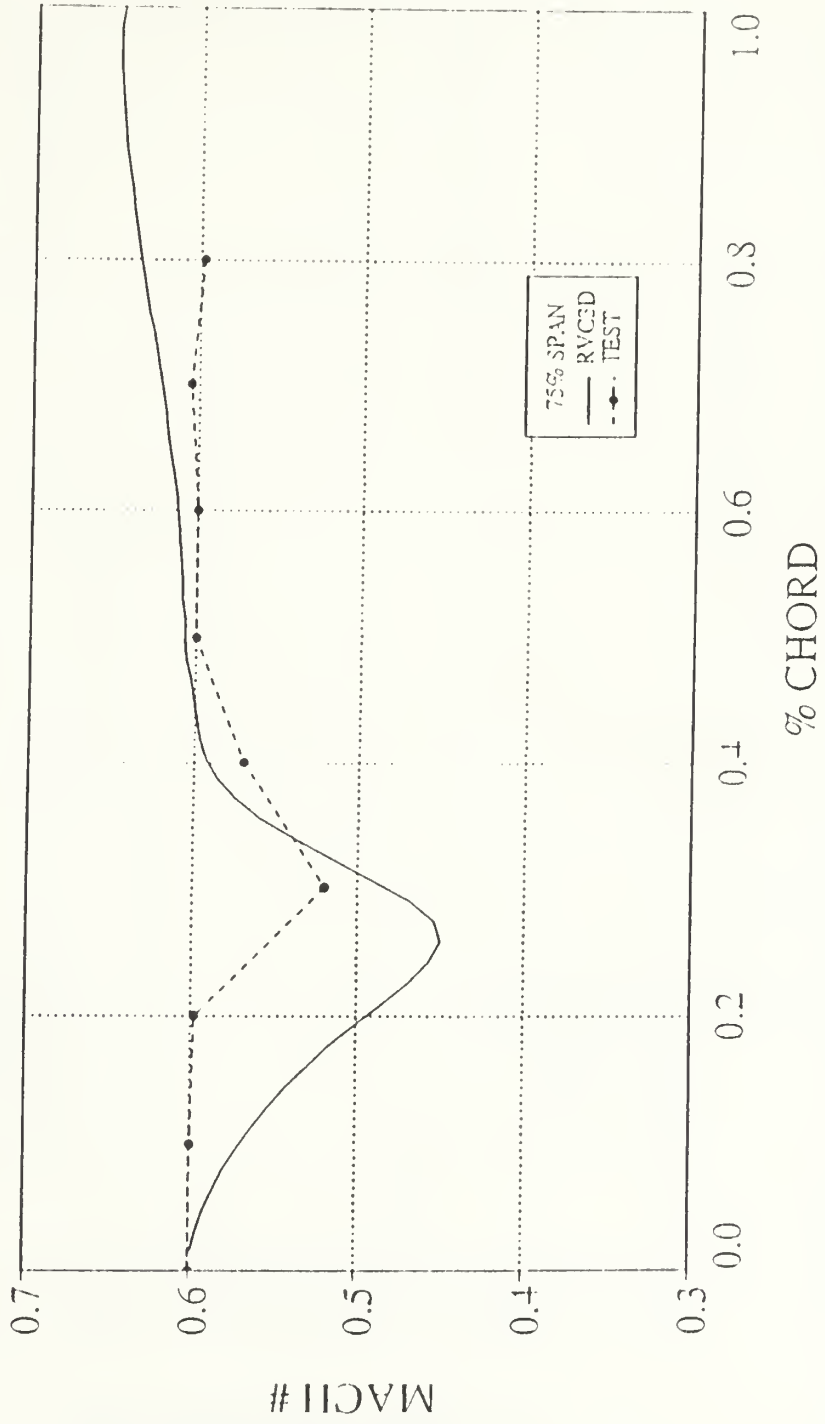
VELOCITY COMPARISON AT 25% SPAN



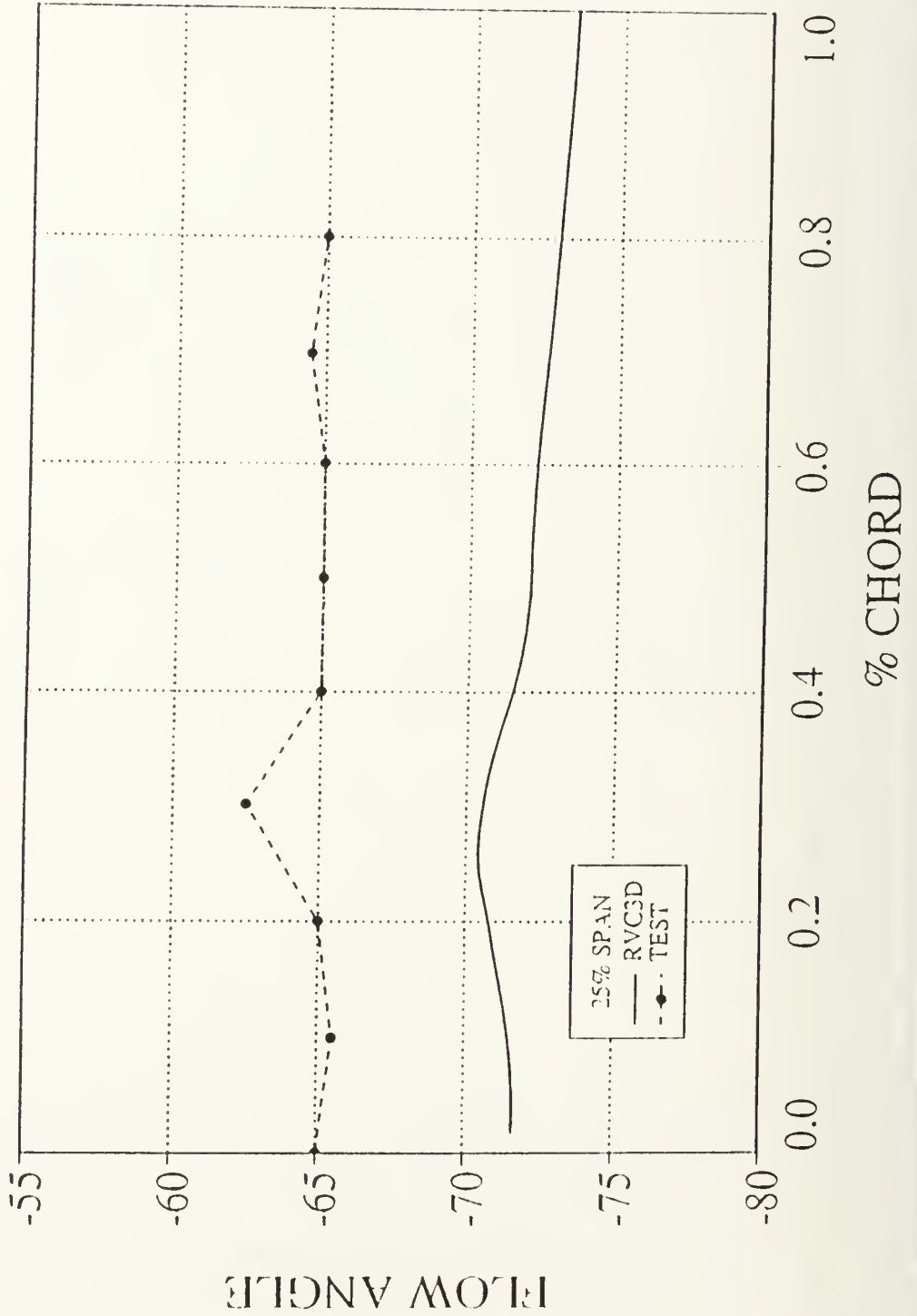
VELOCITY COMPARISON AT 50% SPAN



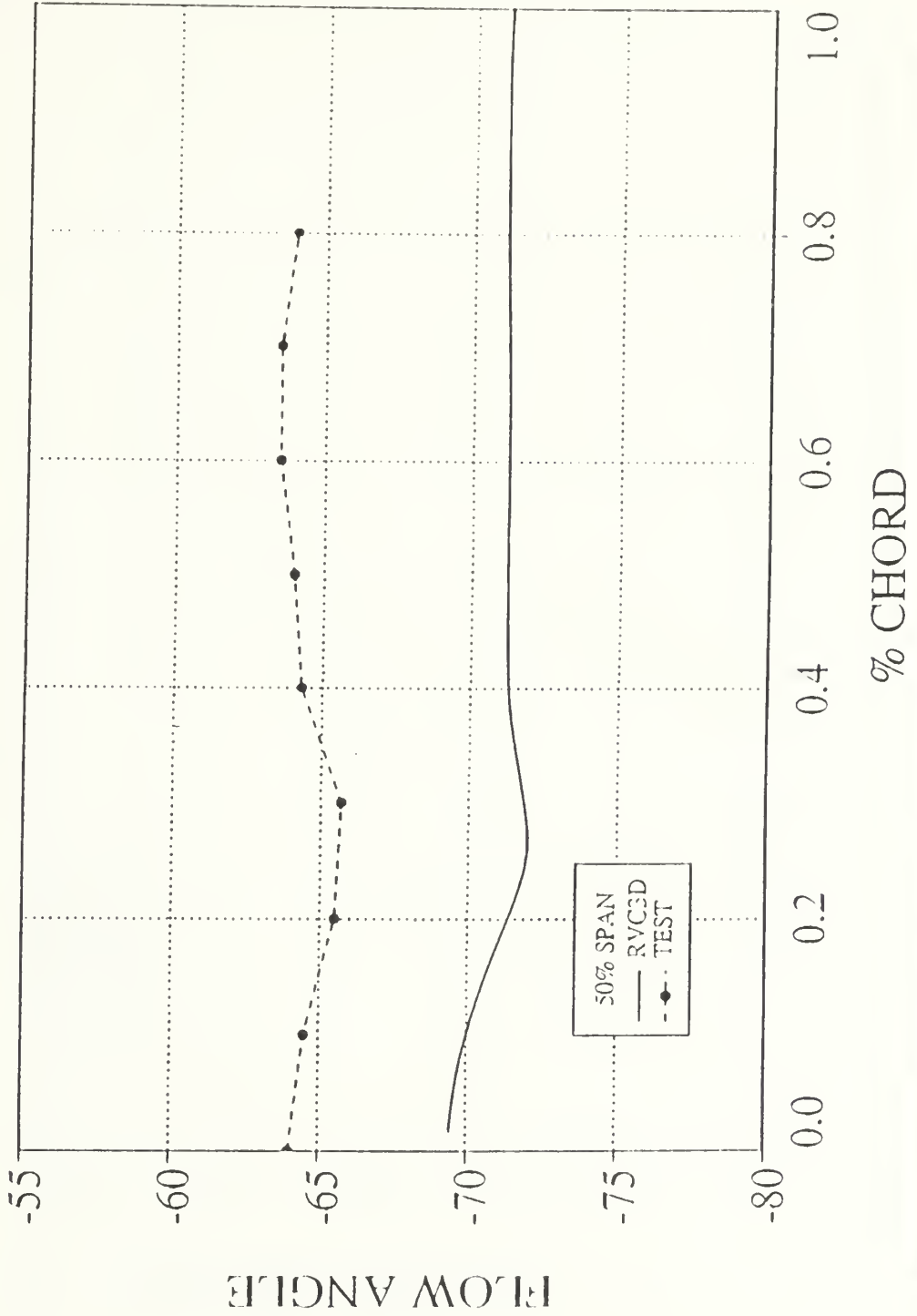
VELOCITY COMPARISON AT 75% SPAN



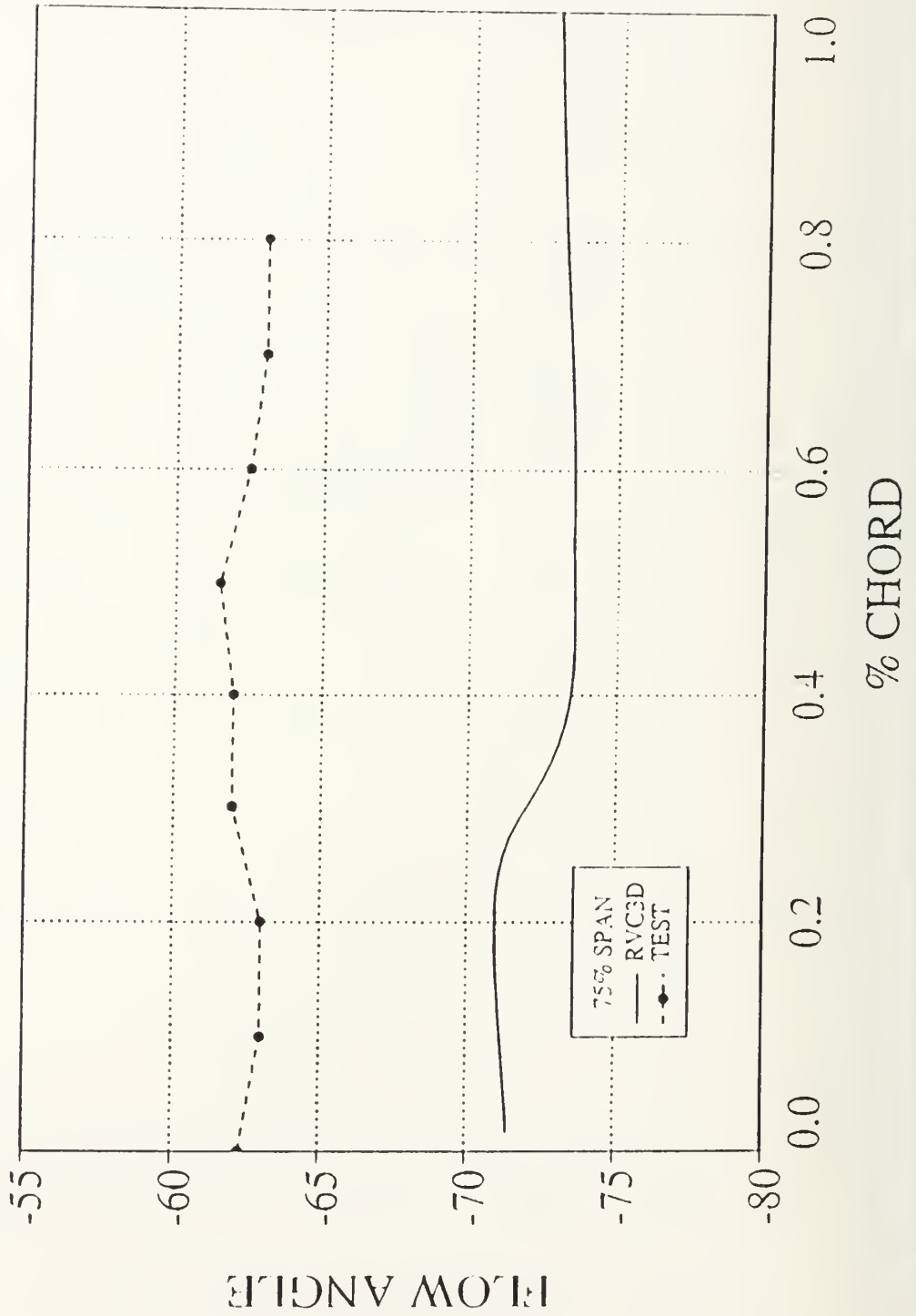
FLOW ANGLE AT 25% SPAN



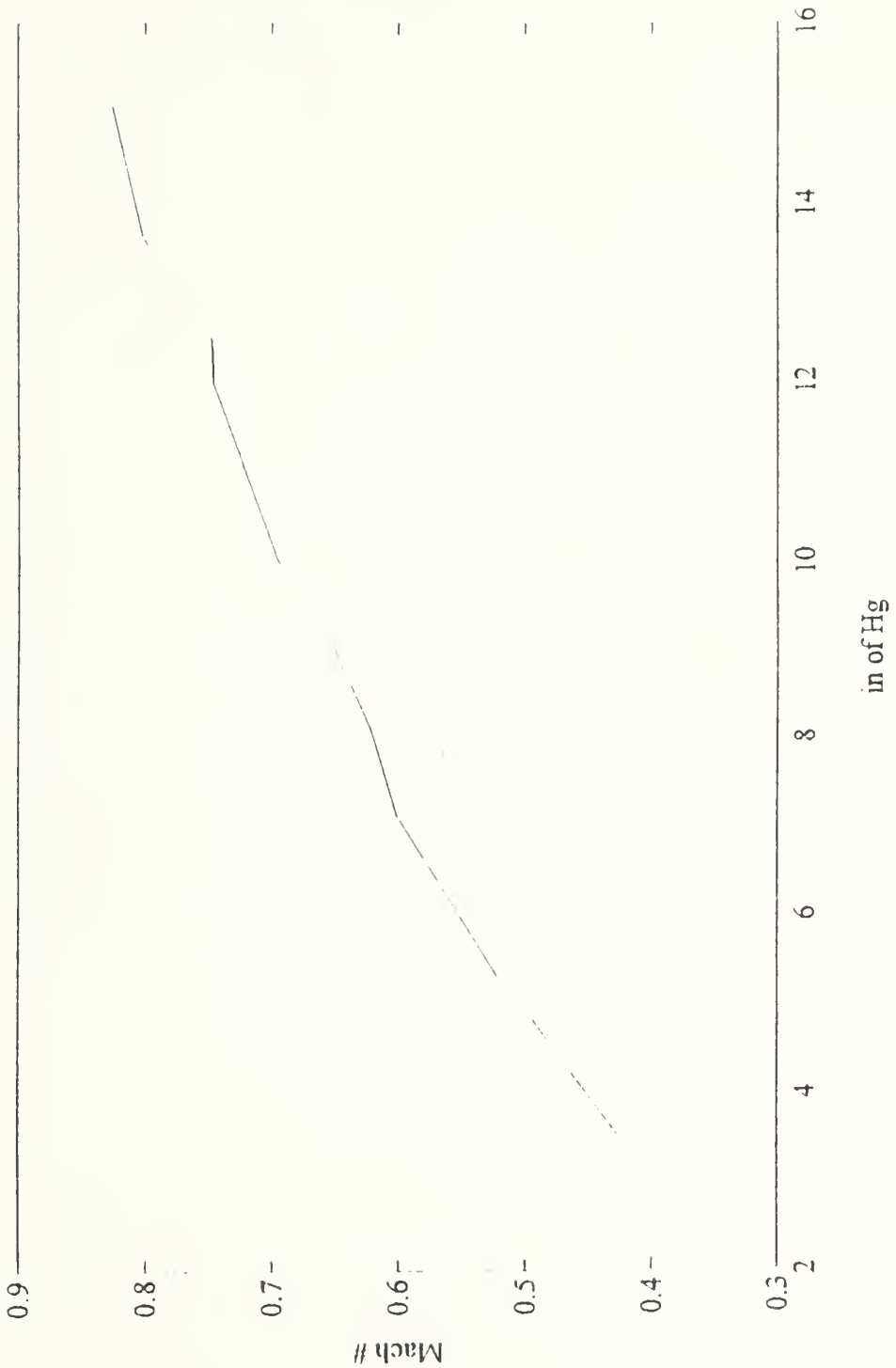
FLOW ANGLE AT 50% SPAN



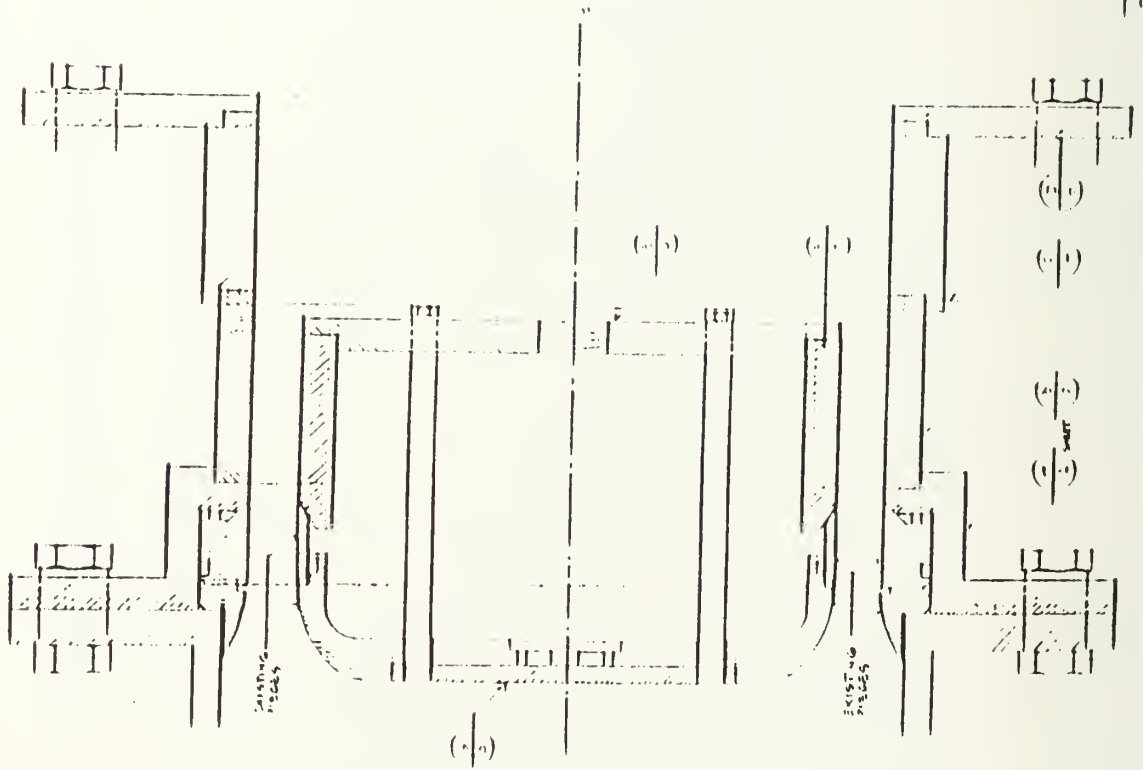
FLOW ANGLE AT 75% SPAN



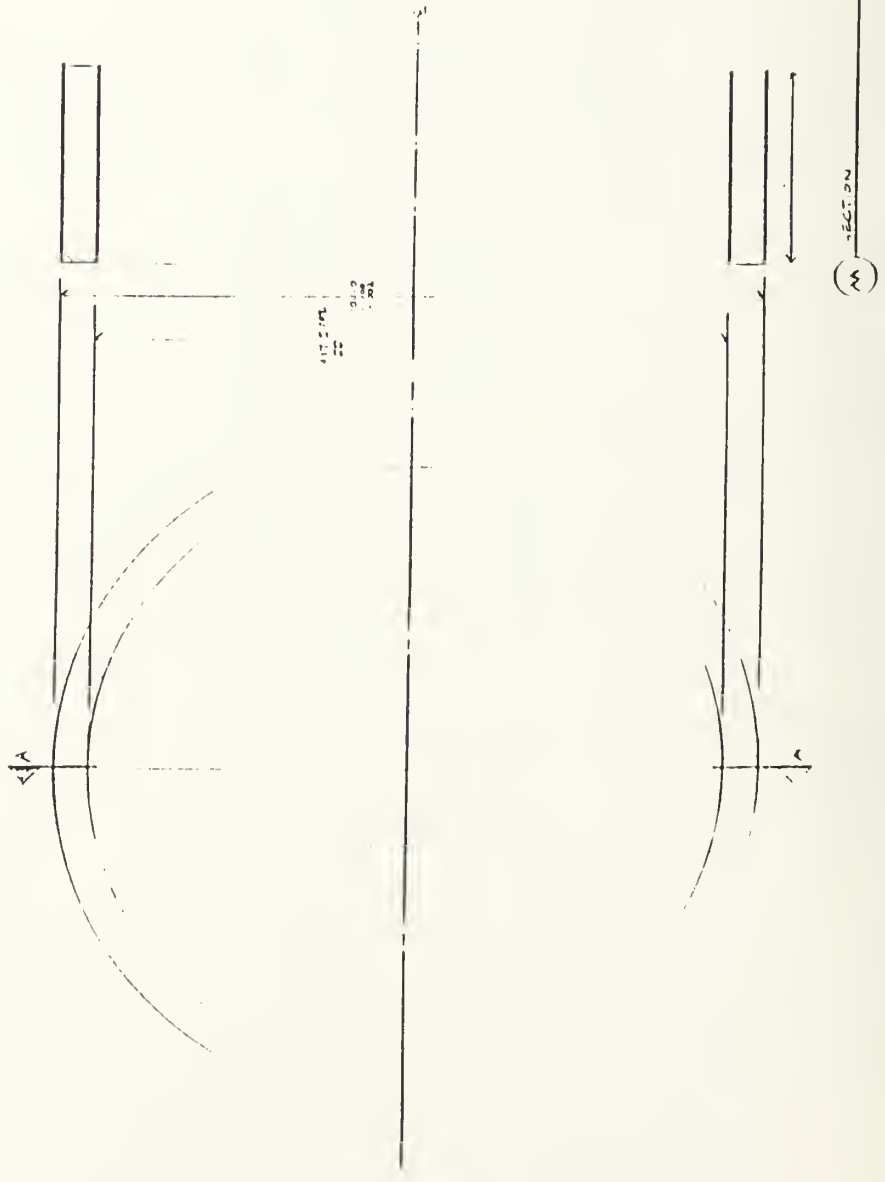
Cobra Probe Calibration



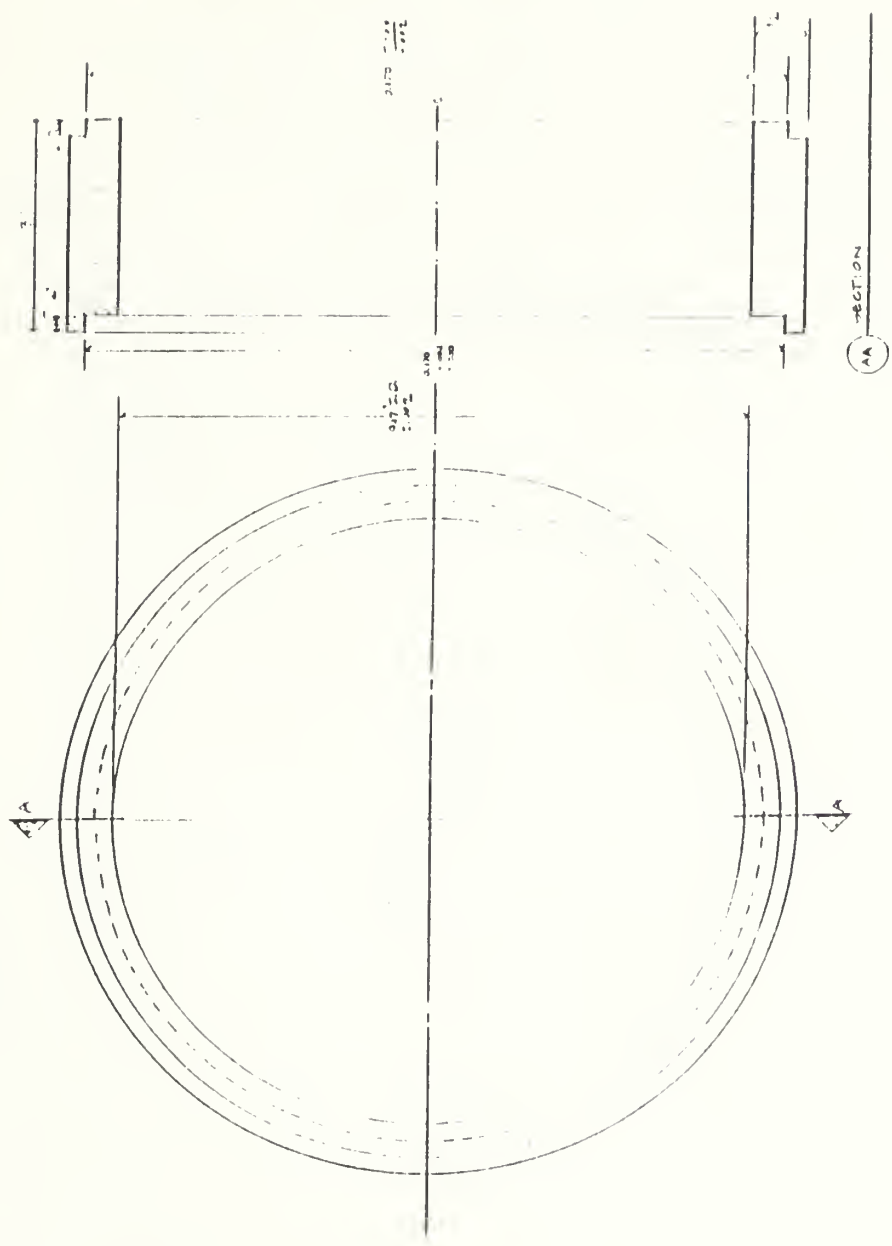
APPENDIX D. DRAWINGS



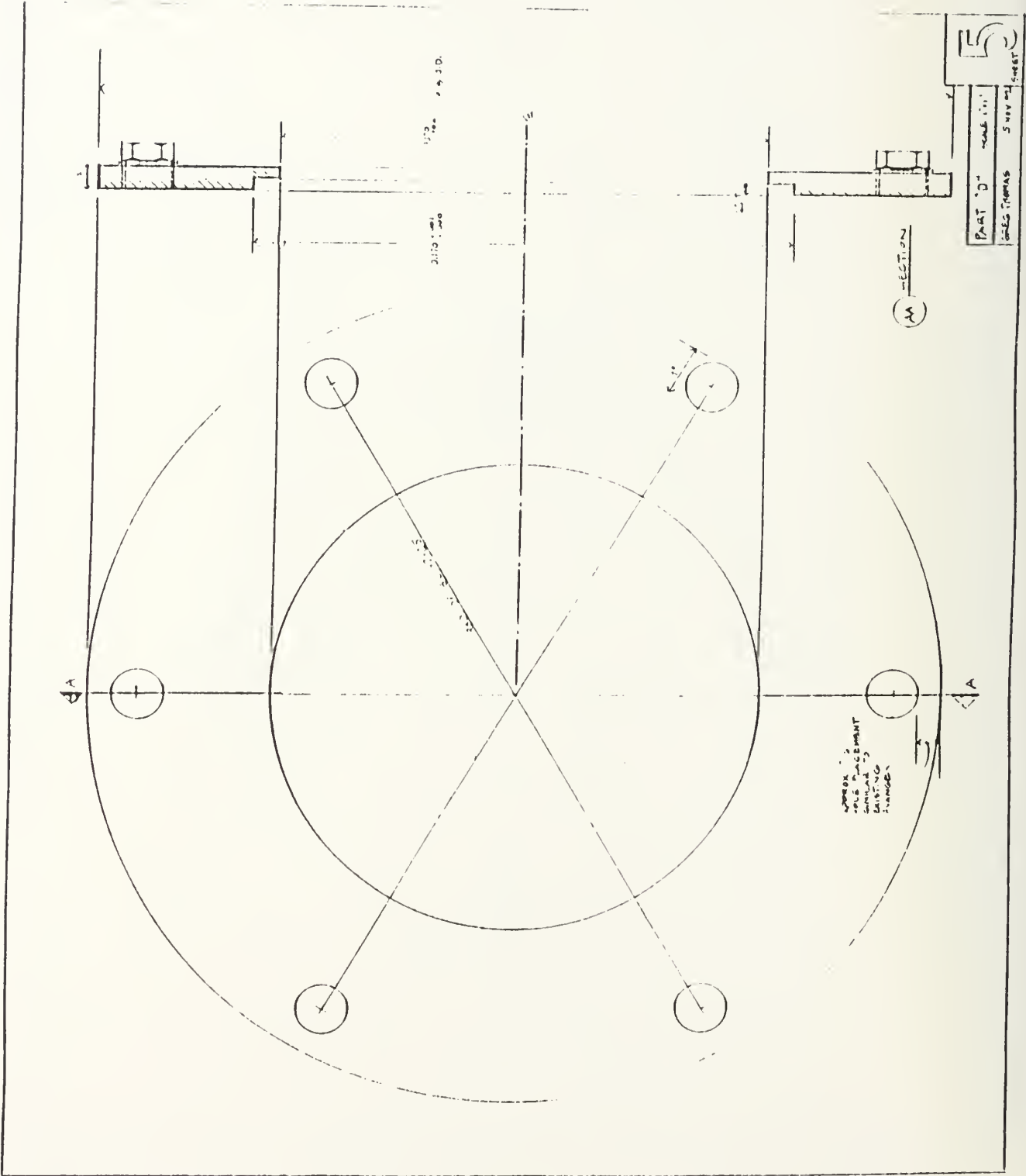
SECTION PARTS
DATE 11/11
M.B.G. (MAY) 1951

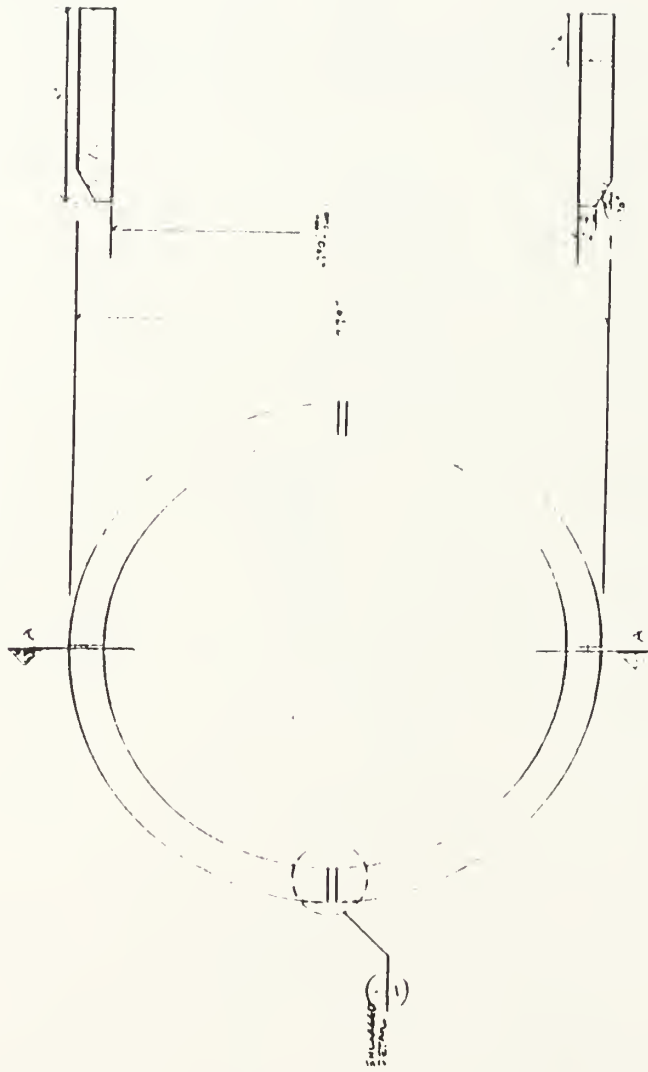


PART "B"
SECTION

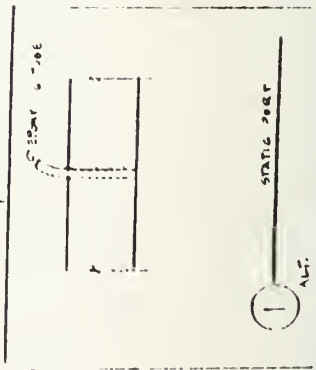


PART "C"
 1941
 JAMES THOMAS - 15 NOV 1941





AA - BOTTOM



1 PART

STATIC PART

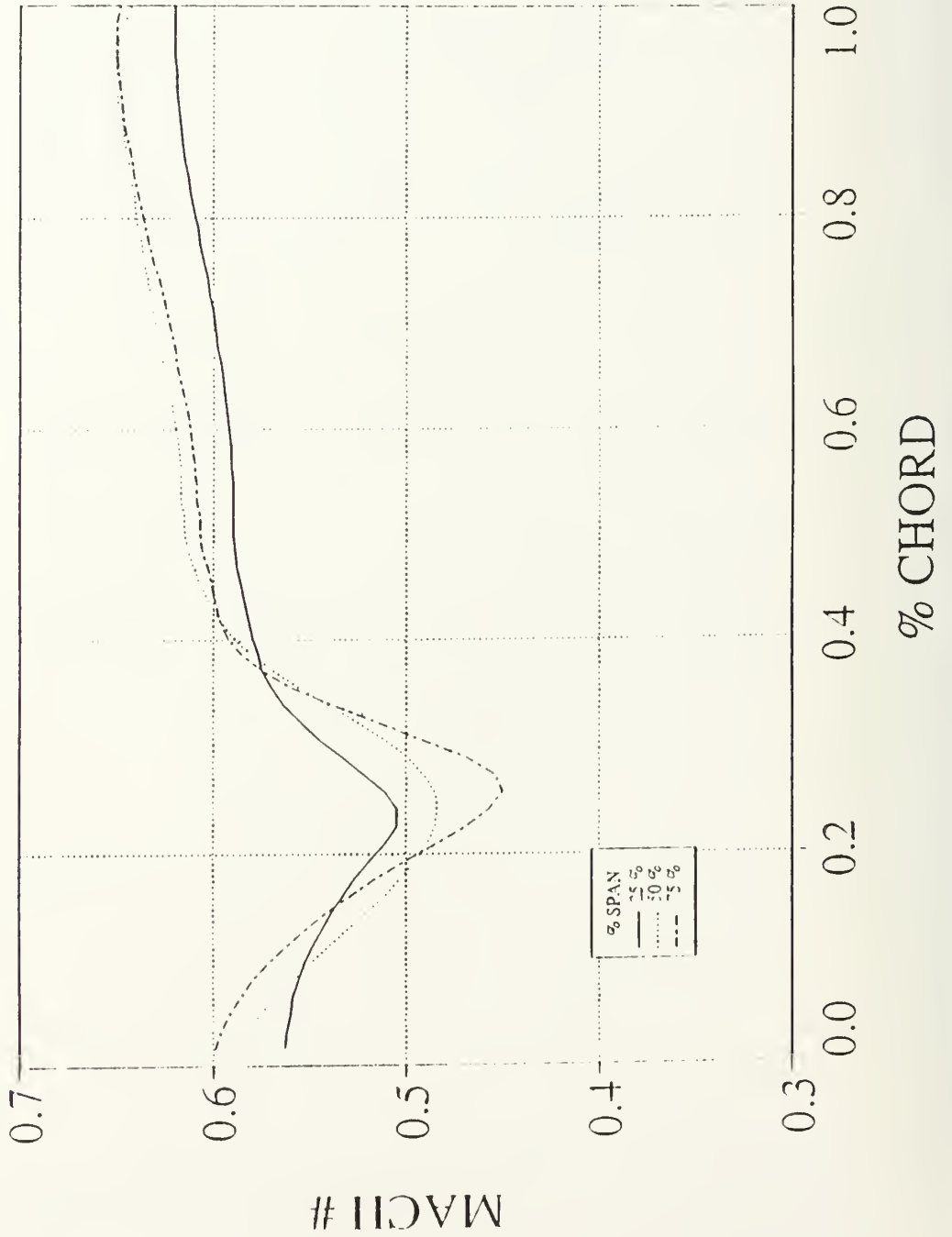
PART 1

SCALE 1:1

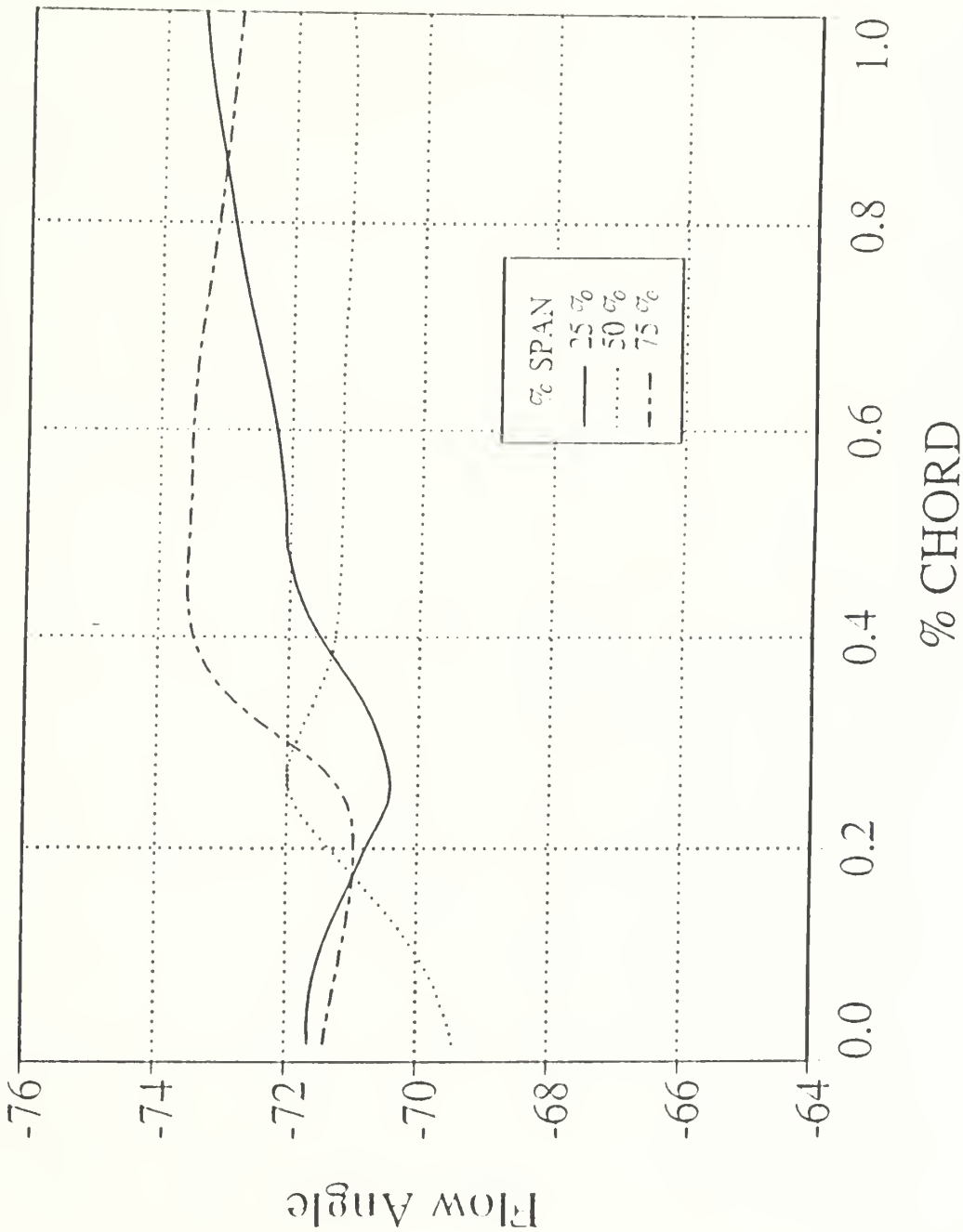
JPEG IMAGES

2 of 21 SHEETS

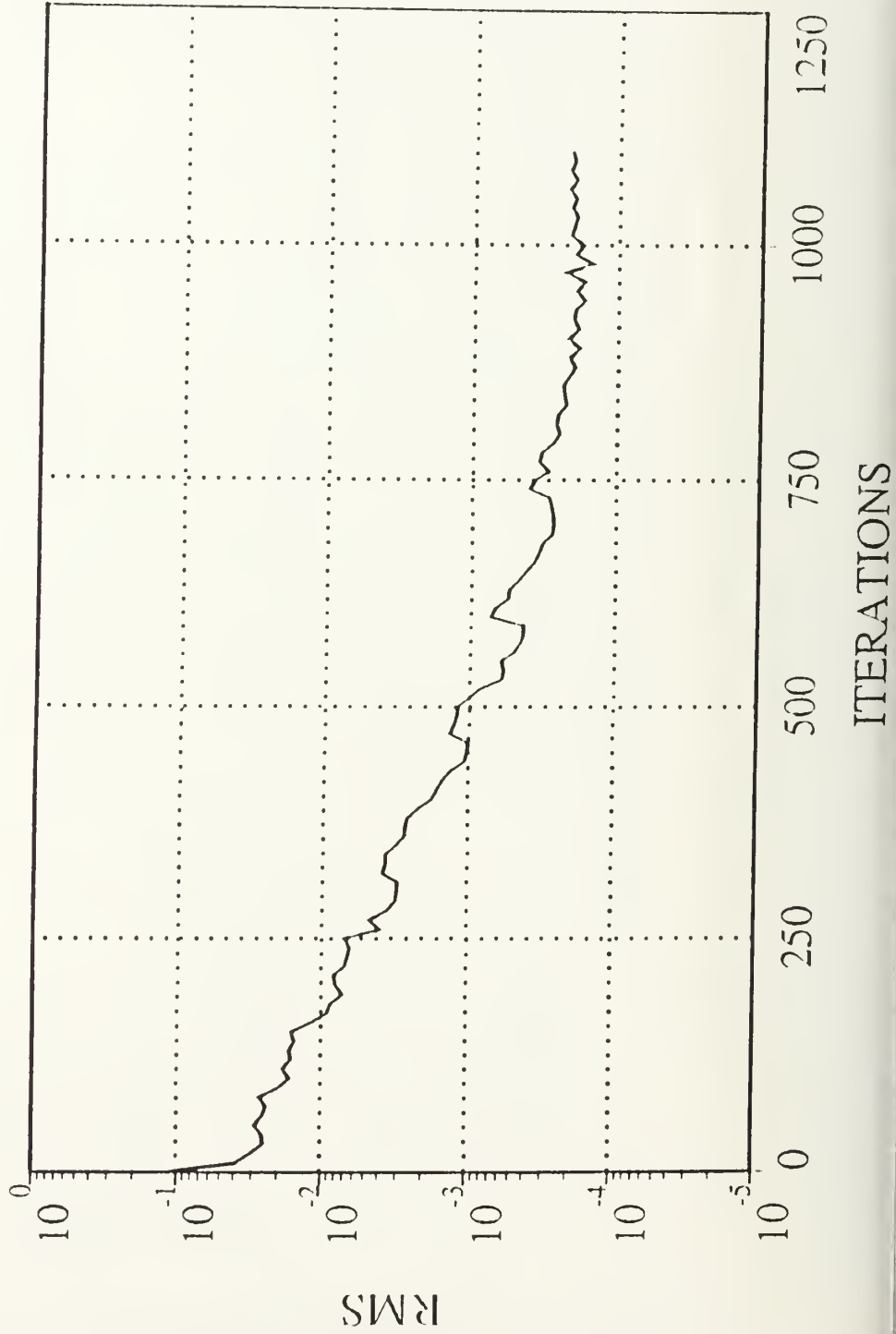
Velocities on Selected Radii



Flow Angles on selected Radii



RESIDUAL HISTORY



APPENDIX F. LDV DATA

May 07 1995

Expt. Ch. (MHz) = 0.000
 Fringe Sp. (pm) = 3.534
 Sample Size = 499.000
 Mean = 76.635
 Std. Dev. = 4.976
 Turb. Int. (Hz) = 6.488

Proc. 1 Data Rate =

1136.44m

Proc. Type :
 Processor Mode :
 Hi Filter :
 Lo Filter :

%

0.0
 0.000 73.584 M/S 147.368

The one component LDV survey data, for mid-span is tabulated below:

Data Point	Velocity (M/S)	Turb. Int. (%)
1	76.848	6.602
2	76.112	6.989
3	76.067	7.328
4	76.246	6.872
5	76.518	7.214
6	75.873	7.841
7	75.908	7.601
8	76.185	7.265
9	76.423	7.190
10	76.256	7.015
11	76.276	7.877
12	76.103	7.766
13	75.889	7.498
14	76.416	7.249
15	76.294	6.992

LIST OF REFERENCES

- [1] Goldman, L. J., and Seasholtz, R. G., "Laser Anemometer Measurements in an Annular Cascade of Core Turbine Vanes and Comparison with Theory," NASA TP-2018, 1982.
- [2] Goldman, L. J., and Seasholtz, R. G., "Laser Anemometer Measurements and Computations in an Annular Cascade of High Turning Core Turbine Vanes," NASA TP-3252, 1992.
- [3] Yamamoto, A., "Production and Development of Secondary Flows and Losses in Two Types Of Straight Turbine Cascades, Part 1-A Stator Case," ASME Journal of Turbomachinery, April 1987, pp. 186-193.
- [4] Chima, R. V., "Viscous Three-Dimensional Calculations of Transonic Fan Performance," AGARD CP-510, AGARD 7th Propulsion and Energetics Panel Symposium on CFD Techniques for Propulsion Applications, San Antonio, TX, May 27-31, 1991. Also NASA TM-103800.
- [5] Dober, D., "Three-Dimensional Fiber-Optic LDV Measurements in the Endwall Region of a Linear Cascade of Controlled-Diffusion Stator Blades," Masters Thesis, Naval Postgraduate School, Monterey, California, March 1993.
- [6] Baldwin, B. S., and Lomax, H., "Thin-Layer Approximation and Algebraic Model for Separated Turbulent Flows." AIAA Paper 78-257, Jan 1978.
- [7] Chima, R. V., Giel, P. W., Boyle, R. J., "An Algebraic Turbulence Model for Three-Dimensional Viscous Flows," in preparation.
- [8] Chima, R. V., Yokota, J. W., "Numerical Analysis of Three-Dimensional Viscous Flows in Turbomachinery," AIAA J., Vol. 28, No. 5, May 1990, pp. 798-806.
- [9] Sorenson, R. L., "A Computer Program to Generate Two-Dimensional Grids About Airfoils and Other Shapes by Use of Poisson's Equation," NASA TM-81198, 1980.

INITIAL DISTRIBUTION LIST

	No. Copies
1. Defense Technical Information Center Cameron Station Alexandria VA 22304-6145	2
2. Library, Code 052 Naval Postgraduate School Monterey CA 93943-5002	2
3. Department Chairman, AA Department of Aeronautics Naval Postgraduate School Monterey, CA 93943	1
4. Garth V. Hobson, Turbopropulsion Laboratory Code AA/Hg Department of Aeronautics Naval Postgraduate School Monterey, CA 93943	5
5. Naval Air Systems Command AIR-536T(Attn: Mr. Paul F. Piscopo) Washington, District of Columbia 20361-5360	1
6. Naval Air Warfare Center Aircraft Division (Trenton) PE-31(Attn: S. Clouser) 250 Phillips Blvd Princeton Crossroads Trenton, NJ 08628-0176	1
7. Gregory D. Thomas 140 Arbusto Circle Sacramento, CA 95831	1

DUDLEY KNOX LIBRARY
NAVAL POSTGRADUATE SCHOOL
MONTEREY CA 93943-5101

DUDLEY KNOX LIBRARY



3 2768 00307439 4